Available online at www.sciencedirect.com
ScienceDirect
Mathematics and Computers in Simulation 205 (2023) 878–901
MATHEMATICS AND COMPUTERS IN SIMULATION
www.elsevier.com/locate/matcom

Original articles

Numerical difference solution of moving boundary random Stefan problems

M.-C. Casabán*, R. Company, L. Jódar

Instituto Universitario de Matemática Multidisciplinar, Building 8G, access C, 2nd floor, Universitat Politècnica de València, Camino de Vera s/n, 46022 Valencia, Spain

Received 5 January 2022; received in revised form 12 September 2022; accepted 21 October 2022
Available online 1 November 2022

Abstract

This paper deals with the construction of numerical solutions of moving boundary random problems where the uncertainty is limited to a finite degree of randomness in the mean square framework. Using a front fixing approach the problem is firstly transformed into a fixed boundary one. Then a random finite difference scheme for both the partial differential equation and the Stefan condition, allows the discretization. Since statistical moments of the approximate stochastic process solution are required, we combine the sample approach of the difference schemes together with Monte Carlo technique to perform manageable approximations of the expectation and variance of both the approximating stochastic process solution and the stochastic moving boundary solution. Qualitative and reliability properties such as positivity, monotonicity and stability in the mean square sense are treated. Feasibility of the proposed method is checked with illustrative examples of a melting problem and a binary metallic alloys problems.

Keywords: Random Stefan problems; Mean square calculus; Front fixing; Finite difference; Finite degree of randomness

1. Introduction

Moving boundary partial differential diffusion problems are frequent modelling phase-change where a material melts or solidifies and they occur in several sciences such as biophysics, chemistry, ecology [6] and industrial processes applications related to melting, freezing [2–4] or metallic alloys processes [1,8,9,12,20].

Apart from the unknown variable of the partial differential equation (PDE), that can be concentration or temperature, it is also important to determine the moving boundary describing the localization of the interface expressed by the Stefan condition.

Dealing with real problems one usually must consider not a deterministic framework but a random one. Such problems are described by random time-dependent PDE models concerning to a wide class of evolution equations, including for instance diffusion–advection–reaction problems. The uncertainty can affect the parameters, coefficients and initial/boundary conditions. There are several sources of uncertainty such as measurement errors, impurities of materials and the difficult to access to the *measurement* of the parameters. In the particular case of random Stefan

* Corresponding author.
E-mail addresses: macabar@imm.upv.es (M.-C. Casabán), rcompany@imm.upv.es (R. Company), ljodar@imm.upv.es (L. Jódar).

https://doi.org/10.1016/j.matcom.2022.10.026

problems the uncertainty arises not only in the searched solution but also in the unknown moving boundary. These issues can be addressed by random or stochastic approaches, based on the mean square (m.s.) calculus [22] or the Itô calculus [15] respectively. Stochastic moving boundary problems have been recently treated in [10,13] using a perturbation approach.

In this paper we address the numerical solution of random moving boundary problems in the m.s. sense. To our knowledge this paper is the first time where random Stefan problems are treated in the m.s. sense. The difficulty to obtain exact solutions suggests the consideration of two problems of increasing complexity.

Since our purpose is numerical we assume a realistic random framework. In our models the involved 2-stochastic processes (s.p.'s) $g(x,t,\omega)$ are defined in a complete probability space $(\Omega,\mathcal{F},\mathbb{P})$. For the sake of practical application we assume that the uncertainty is limited to p degrees of randomness depend on a finite number p of random variables (r.v.'s), see [22, p.37], i.e., they only depend on a finite number p of random variables (r.v.'s)

$$g(x,t,\omega) = g\left(x,t,B_1(\omega),B_2(\omega),\ldots,B_p(\omega)\right), \tag{1}$$

where

$$\left.\begin{array}{l} B_i(\omega),\ 1\le i\le p, \quad \text{are mutually independent r.v.'s,} \\ g \text{ is a differential real function of the variables } x,\ t. \end{array}\right\} \tag{2}$$

This framework has been used recently for random partial differential equations (RPDE) models with fixed domains in [5].

We start with a semi-infinite simple phase random melting problem for which the corresponding deterministic problem has an available exact solution [6, Chpts. 1& 3]:

$$\frac{\partial T(x,t,\omega)}{\partial t} = D(\omega)\,\frac{\partial^2 T(x,t,\omega)}{\partial x^2}, \quad D(\omega)=\frac{\kappa(\omega)}{c_p(\omega)\,\rho(\omega)}, \qquad 0<x=x(t,\omega)<s(t,\omega), \quad \omega\in\Omega, \tag{3}$$

with the following random boundary and initial conditions

$$T(0,t,\omega)=T_{\mathrm{w}}(\omega),\ t>0,\ \omega\in\Omega \text{ (wall temperature)}, \tag{4}$$

$$T(s(t,\omega),t,\omega)=T_{\mathrm{m}}(\omega),\ t>0,\ \omega\in\Omega \text{ (melting front temperature)}, \tag{5}$$

$$T(x,0,\omega)=T_{\mathrm{m}}(\omega),\ x>0,\ \omega\in\Omega \text{ (initial temperature)}, \tag{6}$$

$$s(0,\omega)=0, \quad \omega\in\Omega \qquad \text{(initial position of the interface)}, \tag{7}$$

and the velocity of the 2-stochastic process (2-s.p.) interface $s(t,\omega)$ is stated by a random Stefan condition:

$$\frac{\mathrm{d}s(t,\omega)}{\mathrm{d}t} = -Q(\omega)\left.\frac{\partial T(s(t,\omega),t,\omega)}{\partial x}\right|_{x\to s(t,\omega)^-}, \quad Q(\omega)=\frac{\kappa(\omega)}{L(\omega)\,\rho(\omega)},\ \omega\in\Omega. \tag{8}$$

Here the unknown 2-s.p. $T(x,t,\omega)$, $\omega\in\Omega$, $0<x<s(t,\omega)$, $t>0$, represents the temperature of the material in the liquid phase, $D(\omega)>0$ in (3) represents the diffusivity random variable (r.v.) involving the thermal conductivity r.v. $\kappa(\omega)>0$, the specific heat r.v. $c_p(\omega)>0$ and the density r.v. of the material $\rho(\omega)>0$. The r.v. $Q(\omega)>0$ appearing in the Stefan condition (8) involves the latent heat of fusion r.v. of the phase change material $L(\omega)>0$ and the r.v.'s $\kappa(\omega)>0$ and $\rho(\omega)>0$.

The second problem treated is a diffusional solid-state phase in a binary metallic alloy system [9]

$$C(x,t,\omega)=c^{\mathrm{part}}, \quad 0<x<s(t,\omega),\ \omega\in\Omega, \tag{9}$$

$$\frac{\partial C(x,t,\omega)}{\partial t} = D(\omega)\,\frac{\partial^2 C(x,t,\omega)}{\partial x^2}, \qquad s(t,\omega)<x<\ell, \quad \omega\in\Omega, \tag{10}$$

together with the initial and boundary conditions

$$C(x,0)=\left\{\begin{array}{ll} c^{\mathrm{part}}, & 0\le x<b_0, \\ c^{\mathrm{sol}}, & x=b_0, \\ c^0, & b_0<x\le\ell, \end{array}\right. \tag{11}$$

$$\frac{\partial C(x,t,\omega)}{\partial x}=0\Big|_{x\to\ell^-}, \ \omega\in\Omega, \quad \text{(isolated domain)}, \tag{12}$$

and the random Stefan condition

$$(c^{\text{part}} - c^{\text{sol}}) \frac{\mathrm{d}\, s(t,\omega)}{\mathrm{d}t} = D(\omega) \left. \frac{\partial\, C(x,t,\omega)}{\partial x} \right|_{x \to s(t,\omega)^-}, \quad \omega \in \Omega\,. \tag{13}$$

where $C(x,t,\omega)$ is a 2-s.p. representing the concentration of the material in the diffusive phase $(s(t,\omega), \ell)$. The r.v. $D(\omega) > 0$ denotes the diffusivity inside the diffusive phase. Here c^{part} denotes the concentration within the particle that is assumed to be constant in its domain and b_0 is the initial position of the interface. c^{sol} denotes the constant interface concentration depending on the solubility of the material and c^0 is the initial constant concentration in the diffusive phase. We take $c^{\text{part}} > c^0 > c^{\text{sol}} > 0$.

As it has been mention above in (1)–(2) our models the involved 2-s.p.'s $T(x,t,\omega)$, $C(x,t,\omega)$ and $s(t,\omega)$ are defined in a complete probability space $(\Omega, \mathcal{F}, \mathbb{P})$ and have p degrees of randomness. For the sake of notational simplification we only assume in the example that the involved s.p.'s only depend on one degree of randomness. Additional hypotheses to the involved s.p.'s linked to the m.s. calculus will be imposed later.

Both problems (3)–(8) and (9)–(13) are firstly transformed into a fixed boundary value problem using a random front fixing approach. Then a random finite difference scheme is used to compute both the unknown (temperature or concentration) as well as the melting interface. In order to avoid storage information overload, in the computation of the expectation and the variance of the approximate s.p., we use a combination of the sample m.s. approach with Monte Carlo technique. This combined approach has been recently used in a fixed boundary random partial differential problem where the unmanageable storage information linked to the iteration is overcome [5]. As nothing is perfect, the use of the front-fixing approach so called boundary immobilization method involves a difficulty that must be overcome. In fact, one introduces a singularity derived from the substitution immobilizing the boundary, see later Section 2. See also [19]. Recognized methods as moving grids methods, see [9], can be considered to be applied to the random problem. Recently the unified transform method has been used in the deterministic case leading to integro-differential equations that have been solved numerically by fix-point iteration and spline interpolation, see [7]. In [14] an efficient random walk method has been proposed for the deterministic case. These approaches are worthy to be explored in the random scenario when the parameters are subject to uncertainty. We introduce the front-fixing approach for the considered random Stefan problems inspired in the fact that it has been competitive in the deterministic case [17] and it is used successfully in free boundary problems arising in other fields such as financial mathematics [24] and population dynamics [16].

This paper is organized as follows. Section 2 is devoted to the numerical solution of the random single-phase melting Stefan problem (3)–(8) where under hypotheses (1)–(2) the random exact solution is available. We use a front fixing approach and a random difference scheme where both the melting interface and the temperature become unknowns of the scheme. Numerical results are compared with the exact solution in order to check the reliability of the approach. Numerical analysis is used although not developed to focus more in the innovation since the development is also performed in Section 3. The problem (9)–(2) is treated in Section 3, including the numerical analysis, positivity and qualitative properties of the numerical solution s.p. for both the concentration and the melting interface. Since the exact solution is not available, the reliability of the numerical results are checked using a Cauchy type condition when both the step-sizes and the number of sampled realizations change. A conclusion Section 4 ends the paper.

2. Random single-phase melting Stefan problem

In the random melting Stefan problem (3)–(8) the liquid phase is in contact with a solid phase separated by the unknown melting front at this time, $s(t,\omega)$, $\omega \in \Omega$, where the temperature $T(x,t,\omega)$ is the melting temperature. Initially in $x = 0$, $t = 0$, the wall temperature $T_{\text{w}}(\omega)$ is raised to $T_{\text{w}}(\omega) > T_{\text{m}}(\omega)$, $\omega \in \Omega$, prompting the change of phase to start melting the material. It is important to point out that the single-phase melting problem is an idealization of the two phases problem because in the solid region the temperature is considered to be constantly equal to the melting temperature $T_{\text{m}}(\omega)$. Thus the unknown temperature is only the temperature in the liquid phase, see Fig. 1.

We assume that both s.p.'s the temperature $T(x,t,\omega)$ and the melting interface $s(t,\omega)$ are s.p.'s m.s. differentiable verifying conditions (1)–(2). We assume that the thermophysical properties of the phase change materials are independent of s.p. of the temperature.

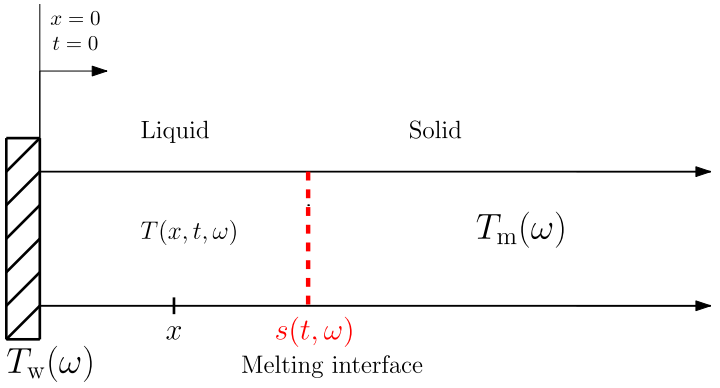

Fig. 1. Schematic of the one-dimensional solid–liquid phase change heat transfer process studied.

In the deterministic case, the Stefan problem described in (3)–(8) in a semi-infinite medium has an analytical solution [6, Chpts. 1 & 3]

$$T(x,t) = T_{\mathrm{w}} - \frac{T_{\mathrm{w}} - T_{\mathrm{m}}}{\operatorname{erf}(\beta)} \operatorname{erf}\left(\frac{x}{2\sqrt{D\,t}}\right), \quad D = \frac{\kappa}{c_p\,\rho}, \quad t > 0, \quad 0 < x < s(t), \tag{14}$$

$$s(t) = 2\beta\sqrt{D\,t}, \quad t \geq 0, \tag{15}$$

where β is the solution of the non-linear equation

$$\beta\, \mathrm{e}^{\beta^2} \operatorname{erf}(\beta) = \frac{Q\ (T_{\mathrm{w}} - T_{\mathrm{m}})}{D\,\sqrt{\pi}}. \tag{16}$$

Note that in the random single-phase melting problem (3)–(8), the spatial variable as it is a proportion of the melting interface $s(t,\omega)$ can be written

$$x(t,\omega) = z\, s(t,\omega), \quad \omega \in \Omega, \tag{17}$$

where z is a real number in the interval $[0,1]$. Hence one achieves Landau transformation [11].

Let us consider the following random front-fixing transformation in order to immobilize the unknown random domain $[0, s(t,\omega)[$

$$z = \frac{x(t,\omega)}{s(t,\omega)}, \quad \omega \in \Omega, \quad t > 0, \tag{18}$$

where z becomes the deterministic spatial variable of the immobilized random boundary problem. The new dependent variable

$$u(z,t,\omega) = T(x(t,\omega),t,\omega), \quad \omega \in \Omega, \tag{19}$$

is the solution s.p. of the random transformed problem

$$\frac{\partial u(z,t,\omega)}{\partial t} = D(\omega)\,\frac{1}{s^2(t,\omega)}\,\frac{\partial^2 u(z,t,\omega)}{\partial z^2} + z\,\frac{s'(t,\omega)}{s(t,\omega)}\,\frac{\partial u(z,t,\omega)}{\partial z}, \quad 0 < z < 1, \quad t > 0, \quad \omega \in \Omega, \tag{20}$$

$$u(0,t,\omega) = T_{\mathrm{w}}(\omega), \ t > 0, \quad \omega \in \Omega, \tag{21}$$

$$u(1,t,\omega) = T_{\mathrm{m}}(\omega), \ t > 0, \quad \omega \in \Omega, \tag{22}$$

$$s(0,\omega) = 0, \quad \omega \in \Omega, \tag{23}$$

$$s'(t,\omega) = -\frac{Q(\omega)}{s(t,\omega)}\ \frac{\partial u(z,t,\omega)}{\partial z}\bigg|_{z\to 1^-}, \ t > 0, \quad \omega \in \Omega, \tag{24}$$

where $s'(t,\omega)$ denotes the first mean square derivative $\frac{\mathrm{d}s(t,\omega)}{\mathrm{d}t}$, $\omega \in \Omega$. Note that immobilization technique involves as an additional variable the melting interface $s(t,\cdot)$ in the transformed random problem (20)–(24).

Remark 1. In order to legitimate the mean square operational calculus developed in (20) and (24) it is important to point out that

$$\frac{\partial^2 u(z,t,\cdot)}{\partial z^2}\,,\quad \frac{\partial u(z,t,\cdot)}{\partial z}\,,\quad \frac{s'(t,\cdot)}{s(t,\cdot)}\,,\quad \frac{1}{s(t,\cdot)}\,,\quad \frac{1}{s^2(t,\cdot)}, \tag{25}$$

lie in $L_4(\Omega)$, see [23, Sec. 3].

As we quoted above it appears the singularity $s(0,\omega)=0$ in (23). Following the idea developed by [19] to circumvent the singularity we use the analytical solution (14)–(16) of the one phase semi-infinite random Stefan Problem in a small initial time interval $0<t<t^0$. Hence from (14)–(16) for the random scenario and the substitution (18)–(19) one gets

$$u(z,t,\omega)=T_{\rm w}(\omega)-\frac{T_{\rm w}(\omega)-T_{\rm m}(\omega)}{\operatorname{erf}(\beta(\omega))}\operatorname{erf}\left(\beta(\omega)\,z\right)\,,\quad 0<t\le t^0\,,\quad 0<z<1\,,\ \omega\in\Omega\,, \tag{26}$$

$$s(t,\omega)=2\beta(\omega)\sqrt{D(\omega)\,t}\,,\quad 0<t\le t^0\,,\ \omega\in\Omega\,, \tag{27}$$

with the r.v. $\beta(\omega)$ the solution of the random non-linear equation

$$\beta(\omega)\,\mathrm{e}^{\beta(\omega)^2}\operatorname{erf}(\beta(\omega))=\frac{Q(\omega)\ (T_{\rm w}(\omega)-T_{\rm m}(\omega))}{D(\omega)\,\sqrt{\pi}}. \tag{28}$$

Let us consider the uniform partition of the spatial domain $[0,1]$ taking a step size h in order to obtain equally spaced points $z_i=ih$, $0\le i\le M$, such that $Mh=1$. For a fixed time τ and a small initial time $t^0>0$, we take a step size k and $N+1$ intermediate time levels are generated $t^n=nk+t^0$, $0\le n\le N$, with $\tau=Nk+t^0$.

We denote the numerical approximation of the s.p.'s $u(z(x,t,\omega),t)$ and $s(t,\omega)$ as follows

$$\begin{array}{rcll} u_i^n(\omega) & \approx & u(z_i,t^n,\omega)\,, & \omega\in\Omega,\quad 0\le i\le M,\ 0\le n\le N\,,\\ s^n(\omega) & \approx & s(t^n,\omega)\,, & \omega\in\Omega,\quad 0\le n\le N\,. \end{array} \tag{29}$$

We proceed with the construction of the random difference scheme (RDS) throughout the approximation of the m.s. derivatives by difference approximations. Concretely the time m.s. derivatives in (20) and (24) are approximated by a forward first-order approximation

$$\frac{\partial u(z(x,t,\omega),t)}{\partial t}\approx\frac{u_i^{n+1}(\omega)-u_i^n(\omega)}{k},\quad \omega\in\Omega, \tag{30}$$

$$s'(t,\omega)\approx\frac{s^{n+1}(\omega)-s^n(\omega)}{k},\quad \omega\in\Omega\,, \tag{31}$$

and by centred second-order approximation for the spatial m.s. partial derivatives in (20)

$$\frac{\partial u(z(x,t,\omega),t)}{\partial z}\approx\frac{u_{i+1}^n(\omega)-u_{i-1}^n(\omega)}{2h}\,,\quad \omega\in\Omega\,, \tag{32}$$

$$\frac{\partial^2 u(z(x,t,\omega),t)}{\partial z^2}\approx\frac{u_{i-1}^n(\omega)-2u_i^n(\omega)+u_{i+1}^n(\omega)}{h^2},\quad \omega\in\Omega\,. \tag{33}$$

Discretization of the Stefan condition (24) involves the approximation of the one size m.s. derivative

$$\left.\frac{\partial u(z,t,\omega)}{\partial z}\right|_{z\to 1^-}\approx\frac{\Delta^n(\omega)}{2h}\,, \tag{34}$$

where

$$\Delta^n(\omega)=3u_M^n(\omega)-4u_{M-1}^n(\omega)+u_{M-2}^n(\omega)\,, \tag{35}$$

preserving the second order approximation as the approximation of the m.s. derivatives at the internal points. Using that the melting interface follows the evolution of the transformed Stefan condition (24) and expressions (15), (34)–(35) one gets

$$\left.\begin{array}{rcll} s^{n+1}(\omega) & = & s^n(\omega)-\dfrac{k\ Q(\omega)\ \Delta^n(\omega)}{s^n(\omega)\,2h}\,, & 0\le n\le N-1\,,\\ s^0(\omega) & = & 2\,\beta(\omega)\,\sqrt{D(\omega)\,t^0}\,, & t^0>0\,, \end{array}\right\}\,,\ \omega\in\Omega\,. \tag{36}$$

By the approximations (30)–(35) the random problem (20)–(24) can be rewritten as the following random discretized front-fixing problem

$$\left.\begin{aligned} \frac{u_i^{n+1}(\omega)-u_i^n(\omega)}{k} = \\ D(\omega)\frac{u_{i-1}^n(\omega)-2u_i^n(\omega)+u_{i+1}^n(\omega)}{(s^n(\omega))^2\ h^2} - \frac{Q(\omega)\,\Delta^n(\omega)}{4(s^n(\omega))^2\,h^2}\left(u_{i+1}^n(\omega)-u_{i-1}^n(\omega)\right)\ z_i\,, \\ 1\le i\le M-1,\ 0\le n\le N-1\,, \\ u_0^n(\omega)=T_{\rm w}(\omega)\,,\quad u_M^n(\omega)=T_{\rm m}(\omega)\,,\quad 0\le n\le N\,, \\ u_i^0(\omega)=\frac{T_{\rm m}(\omega)-T_{\rm w}(\omega)}{\operatorname{erf}(\beta)}\operatorname{erf}(\beta\, z_i)+T_{\rm w}(\omega)\,,\quad 0\le i\le M\,. \end{aligned}\right\} \tag{37}$$

Note that the initial condition of the RDS (37), $\{u_i^0(\omega)\ ;\ 0\le i\le M,\ \omega\in\Omega\}$, is obtained from the evaluation (26) at time $t=t^0$.

The random explicit scheme constructed takes the form

$$\left.\begin{aligned} u_i^{n+1}(\omega)=a_i^n(\omega)\,u_{i-1}^n(\omega)+b^n(\omega)\,u_i^n(\omega)+c_i^n(\omega)\,u_{i+1}^n\,,\quad \omega\in\Omega\,, \\ 1\le i\le M-1,\ 0\le n\le N-1\,, \\ u_0^n(\omega)=T_{\rm w}(\omega)\,,\quad u_M^n(\omega)=T_{\rm m}(\omega)\,,\quad 0\le n\le N\,, \\ u_i^0(\omega)=\frac{T_{\rm m}(\omega)-T_{\rm w}(\omega)}{\operatorname{erf}(\beta(\omega))}\operatorname{erf}(\beta(\omega)\,z_i)+T_{\rm w}(\omega)\,,\quad 0\le i\le M\,. \end{aligned}\right\} \tag{38}$$

with the random coefficients

$$\left.\begin{aligned} a_i^n(\omega)=\frac{k}{h^2(s^n(\omega))^2}\left(D(\omega)+\frac{Q(\omega)\,\Delta^n(\omega)}{4}z_i\right) \\ b^n(\omega)=1-\frac{2k\,D(\omega)}{h^2\,(s^n(\omega))^2} \\ c_i^n(\omega)=\frac{k}{h^2(s^n(\omega))^2}\left(D(\omega)-\frac{Q(\omega)\,\Delta^n(\omega)}{4}z_i\right) \end{aligned}\right\}\quad 1\le i\le M-1,\quad 0\le n\le N-1\,,\ \omega\in\Omega\,, \tag{39}$$

and $\Delta^n(\omega)$ defined in (35).

In an analogous way to the further study of the m.s. stability developed in Section 3, and to avoid straightforward computations, it is easy to show that for small enough values of the step-size h together with the hypothesis

$$\frac{k}{h^2}<2\,t^0\,\beta_{\min}^2\,, \tag{40}$$

where $\beta_{\min}=\min\{\beta(\omega):\omega\in\Omega\}$, one guarantees the positivity and stability of the solution s.p. of the RDS (35)–(36), (38)–(39) and the time increasing behaviour of the melting interface s.p. obtained from (36).

In the next example as the exact solution is available we compare this one with the random solution s.p. of the RDS as well as their statistical moments using Monte Carlo technique only at the fixed station time iteration to avoid storage-accumulation troubles, see [5].

2.1. Example: Simulation of the random ice melting in a single-phase

In order to illustrate and validate the random solid–liquid phase change simulation results obtained in our study, we are going to consider a block of ice of negligible thickness. Table 1 collects the physical values for the parameters involved in the problem according with the standard reference data in the literature, see for instance [18,21]. The data taken have been considered mutually independent. We denote $N_{[a,b]}(\mu,\sigma)$ the normal distribution of mean μ and standard deviation σ truncated in the interval $[a,b]$. We have chosen truncated normal distributions for the

Table 1
Thermophysical properties of water and other data of Example 2.1.

Parameter	Physical value	Unit
T_w	10	°C
T_m	0	°C
Thermal Conductivity ($\kappa(\omega)$)	$\kappa(\omega) \sim N_{[0.5,0.7]}(0.60, 0.10)$	W/(m °C)
Density of the liquid (ρ)	1000	g/l
Specific heat (c_p)	4.1868	J/(g °C)
$D(\omega) = \dfrac{\kappa(\omega)}{c_p\,\rho}$	$D(\omega) = 14.3308\,\kappa(\omega)$	mm^2/min
Latent heat of fusion ($L(\omega)$)	$L(\omega) \sim N_{[0.31,0.35]}(0.33, 0.02)$	KJ/g
$Q(\omega) = \dfrac{\kappa(\omega)}{L(\omega)\,\rho}$	$Q(\omega) = 6 \times 10^{-2}\dfrac{\kappa(\omega)}{L(\omega)}$	mm^2/(°C min)

random parameters inspired in the fact that this distribution is generally expected to describe errors of measurement but any other truncated one can be used for our proposed random front-fixing numerical scheme. The values of the means of the parameters have been taken as approximations of the standard physical reference data of $\kappa(\omega)$ and $L(\omega)$ respectively. Although the choice of the distributions and their parameters modifies the numerical solutions it is worth focusing on the fact that stability is guaranteed in all the cases if the condition between the step sizes discretization (40) is assumed.

With respect to the computations of the mean and the standard deviation of the exact solution s.p. (14)–(16), we need to overcome the trouble of solving for $\beta(\omega)$, $\omega \in \Omega$, the random non-linear equation (28). Taking a high number of sampled realizations in (28) and solving the corresponding sampled equations, then each sampled solution $\beta(\omega_K)$ is taking in the transformed problem (26)–(27) in order to compute the mean and the standard deviation of the solution s.p. $u(z,t,\omega)$ of (26) and $s(t,\omega)$ of (27). The transformation (17)–(18) allows us to compute the mean of the r.v. $x(t,\cdot)$ at a fixed time t,

$$\mu[x(t,\omega)] = z\ \mu[s(t,\omega)]\,, \quad 0 \le z \le 1\,. \tag{41}$$

Finally the mean of the temperature above computed $\mu[u(z,t,\omega)]$ is assigned to the mean of the space variable $\mu[x(t,\omega)]$ given by (41). As $\sigma[x(t,\omega)] = z\ \sigma[s(t,\omega)]$, the same spatial assignation is performed with respect to the standard deviation. This procedure is valid for both the exact and the numerical solution s.p.'s. Algorithm 1 summarizes the sufficient conditions and steps to compute stable approximations for both statistical moments of the solution s.p.'s temperature and interface generated by means of the random difference scheme (35)–(36), (38)–(39) and the Monte Carlo method.

The comparison among theirs statistical moments is performed for the real spatial variable z at a fixed time τ, using (26)–(27) for the exact solution and (35)–(36), (38)–(39) for the numerical one from t^0 up to τ. The study of the numerical convergence of these approximations has been treated by means of the analysis of their absolute errors in two stages at a fixed time τ. Firstly, we have fixed the step-sizes (h,k) verifying the sufficient stability condition (40) and we have varied the number K of Monte Carlo realizations comparing their absolute differences between two successive realizations $\{K_\ell, K_{\ell+1}\}$ using the following expressions

$$\begin{aligned}
\text{AbsDiff}\left[\mu\left(u_{K_\ell K_{\ell+1}}(z_i,\tau,\omega)\right)\right] &= \left|\text{AbsErr}\left[\mu\left(u_{K_{\ell+1}}(z_i,\tau,\omega)\right)\right] - \text{AbsErr}\left[\mu\left(u_{K_\ell}(z_i,\tau,\omega)\right)\right]\right|,\\
\text{AbsDiff}\left[\sigma\left(u_{K_\ell K_{\ell+1}}(z_i,\tau,\omega)\right)\right] &= \left|\text{AbsErr}\left[\sigma\left(u_{K_{\ell+1}}(z_i,\tau,\omega)\right)\right] - \text{AbsErr}\left[\sigma\left(u_{K_\ell}(z_i,\tau,\omega)\right)\right]\right|,
\end{aligned} \tag{42}$$

$$\begin{aligned}
\text{AbsDiff}\left[\mu\left(s_{K_\ell K_{\ell+1}}(t^n,\omega)\right)\right] &= \left|\text{AbsErr}\left[\mu\left(s_{K_{\ell+1}}(t^n,\omega)\right)\right] - \text{AbsErr}\left[\mu\left(s_{K_\ell}(t^n,\omega)\right)\right]\right|,\\
\text{AbsDiff}\left[\sigma\left(s_{K_\ell K_{\ell+1}}(t^n,\omega)\right)\right] &= \left|\text{AbsErr}\left[\sigma\left(s_{K_{\ell+1}}(t^n,\omega)\right)\right] - \text{AbsErr}\left[\sigma\left(s_{K_\ell}(t^n,\omega)\right)\right]\right|,
\end{aligned} \tag{43}$$

where the absolute errors of the mean and the standard deviation between the exact values, $u(z_i,\tau,\omega)$ and $s(t^n,\omega)$, and the approximate ones denoted by $u_K(z_i,\tau,\omega)$ and $s_K(t^n,\omega)$, are computed in this way

$$\begin{aligned}
\text{AbsErr}\left[\mu\left(u_K(z_i,\tau,\omega)\right)\right] &= \left|\mu\left(u(z_i,\tau,\omega)\right) - \mu\left(u_K(z_i,\tau,\omega)\right)\right|,\\
\text{AbsErr}\left[\sigma\left(u_K(z_i,\tau,\omega)\right)\right] &= \left|\sigma\left(u(z_i,\tau,\omega)\right) - \sigma\left(u_K(z_i,\tau,\omega)\right)\right|,\\
\text{AbsErr}\left[\mu\left(s_K(t^n,\omega)\right)\right] &= \left|\mu\left(s(t^n,\omega)\right) - \mu\left(s_K(t^n,\omega)\right)\right|,\\
\text{AbsErr}\left[\sigma\left(s_K(t^n,\omega)\right)\right] &= \left|\sigma\left(s(t^n,\omega)\right) - \sigma\left(s_K(t^n,\omega)\right)\right|.
\end{aligned} \tag{44}$$

Algorithm 1 Procedure to compute the statistical moments of the numerical solutions s.p.'s $u_i^n(\omega)$ and $s^n(\omega)$, $\omega \in \Omega$, for the random transformed problem (20)–(24) in Example 2.1. **(Part 1)**

Assume that both numerical solution s.p.'s $u_i^n(\omega)$ and $s^n(\omega)$ are in $L_4(\Omega)$ space verifying conditions (1)–(2) and (25).

Take random inputs $\kappa(\omega)$ and $L(\omega)$ as truncated r.v.'s.

Select a uniform spatial step-size h generating the nodes $z_i = i\,h$, $0 \leq i \leq M$, in $[0, 1]$ such that $Mh = 1$.

Choose a fixed time τ and a small initial time $t^0 > 0$.

Consider the maximum value of the latent heat of fusion r.v. $L(\omega)$ in order to obtain $\beta_{\min}$, that is, the minimum value of r.v. $\beta(\omega)$ in (28) for any event ω.

Select a temporal step-size k verifying condition (40).

Consider a partition of the temporal interval $[t^0, \tau]$ of the form $t^n = n\,k + t^0$, $0 \leq n \leq N$, where the integer $N = \frac{\tau - t^0}{k}$ is the number of levels necessary to achieve the time τ, that is, $\tau = Nk + t^0$.

Take an integer number K of Monte Carlo realizations, ω_ℓ, $1 \leq \ell \leq K$, over the r.v.'s obtaining the real values $\kappa(\omega_\ell)$ and $L(\omega_\ell)$, $1 \leq \ell \leq K$.

for each realization ω_ℓ, $1 \leq \ell \leq K$ **do**
  Compute the deterministic root $\beta(\omega_\ell)$ of the non-linear deterministic equation associated to (28).
  for $n = 0$ **do**
    for $i = 1$ to $M - 1$ **do**
      Compute the initial solution $u_i^0(\omega_\ell)$ at $t^0 > 0$ using (38).
    end for
  end for

  for $n = 1$ **do**
    Compute $\Delta^0(\omega_\ell)$ using (35).
    Compute $s^0(\omega_\ell)$ using (36).
    Compute $b^0(\omega_\ell)$ using (39)
    for $i = 1$ to $M - 1$ **do**
      Compute coefficients $a_i^0(\omega_\ell)$ and $c_i^0(\omega_\ell)$ using (39).
      Compute $u_i^1(\omega_\ell)$ using (38).
    end for
  end for

  for $n = 2$ to $n = N$ **do**
    Compute $\Delta^{n-1}(\omega_\ell)$ using (35).
    Compute $s^{n-1}(\omega_\ell)$ using (36).
    Compute $b^{n-1}(\omega_\ell)$ using (39)
    for $i = 1$ to $M - 1$ **do**
      Compute coefficients $a_i^{n-1}(\omega_\ell)$ and $c_i^{n-1}(\omega_\ell)$ using (39).
      Compute $u_i^n(\omega_\ell)$ using (38).
    end for
  end for

  Compute $\Delta^N(\omega_\ell)$ using (35).
  Compute $s^N(\omega_\ell)$ using (36).
end for

Algorithm 1 (Part 2)

1: **for** $i = 1$ to $M - 1$ **do**
2: Compute the mean of the numerical temperature solutions at time level N over the set of the K realizations: $\mu[u_i^N(\omega_\ell), 1 \leq \ell \leq K]$.
3: Compute the standard deviation of the numerical temperature solutions at time level N over the set of the K realizations: $\sigma[u_i^N(\omega_\ell), 1 \leq \ell \leq K]$.
4: **end for**
5: **for** $n = 1$ to N **do**
6: Compute the mean of the numerical interface solutions over the set of the K realizations: $\mu[s^n(\omega_\ell), 1 \leq \ell \leq K]$.
7: Compute the standard deviation of the numerical interface solutions over the set of the K realizations: $\sigma[s^n(\omega_\ell), 1 \leq \ell \leq K]$.
8: **end for**

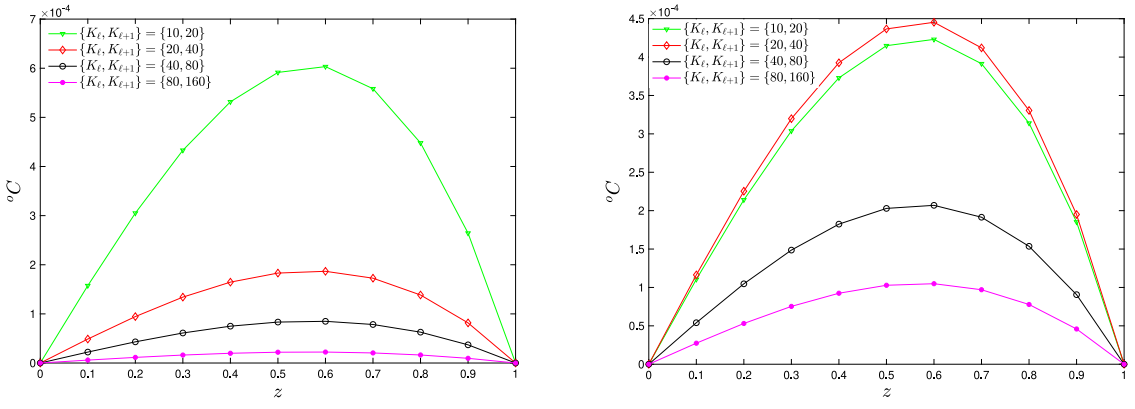

Fig. 2. Absolute differences after $\tau = 5.5$ min for both statistical moments of the approximate temperature s.p., $u_{K_\ell, K_{\ell+1}}(z, \tau, \omega)$, computed by (42) between two successive realizations $\{K_\ell, K_{\ell+1}\}$, $K_\ell \in \{10, 20, 40, 80, 160\}$. The step-sizes $(h, k) = (0.1, 5\text{e}-04)$ are considered fixed, then the spatial points are $z_i = ih$, $1 \leq i \leq M - 1 = 10$ in the spatial domain $[0, 1]$. Plot (a): Successive absolute differences of the mean of the approximate temperature s.p.: $\text{AbsDiff}\left[\mu\left(u_{K_\ell K_{\ell+1}}(z, 5.5, \omega)\right)\right]$. Plot (b): Successive absolute differences for the standard deviation of the approximate temperature s.p.: $\text{AbsDiff}\left[\sigma\left(u_{K_\ell K_{\ell+1}}(z, 5.5, \omega)\right)\right]$.

Figs. 2 and 3 show how the successive absolute differences (42)–(43) decrease as the number of Monte Carlo realizations $K_\ell \in \{10, 20, 40, 80, 160\}$ increases for the fixed step-sizes $(h, k) = (0.1, 5\text{e}-04)$. Tables 2 and 3 collect the maximum values of these absolute differences. Computations have been carried out by Matlab© software version R2019b Update 3 for Windows 10Pro (64-bit) AMD Ryzen Threadripper 2990WX 32-Core Processor, 3.00 GHz. The timings have been computed using cputime function of Matlab© (CPU time spent). Table 4 collects these CPUs as well as the real time lapsed corresponding to these CPUs.

In the second stage about the study of the convergence of the approximations to the both statistical moments, we have taken a fixed number of Monte Carlo realizations K, $K = 500$, and we have refined the step-sizes (h, k) according to the stability condition (40). Figs. 4 and 5 illustrate the behaviour of the absolute errors as the step sizes decrease up to the values $(h, k) = (0.025, 3.5\text{e}-05)$. The absolute errors decrease in the case of the mean and remain stable for the case of the standard deviation. Tables 5 and 6 collect the maximum value for these absolute errors and Table 7 collects the CPUs and the real time lapsed in the computations of the mean and the standard deviation.

Fig. 6 shows wrong numerical approximations obtained when the sufficient stability condition (40) is broken. In fact, considering the spatial step-size $h = 0.025$, the initial time $t^0 = 0.5$ minutes, the final time $\tau = 5.5$ minutes,

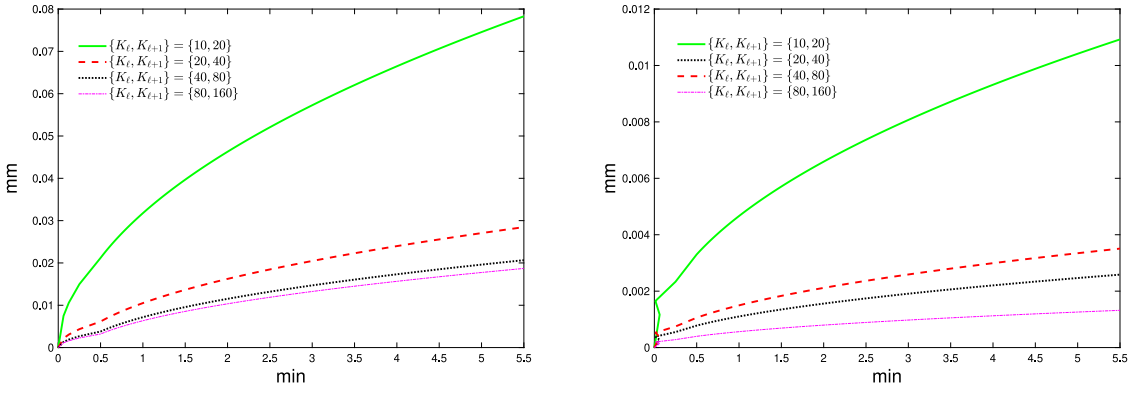

Fig. 3. Absolute differences over the $\tau = 5.5$ min for both statistical moments of the approximate melting interface s.p. computed by (43) between two successive realizations $\{K_\ell, K_{\ell+1}\}$, $K_\ell \in \{10, 20, 40, 80, 160\}$. The step-sizes $(h, k) = (0.1, 5e-04)$ are considered fixed, then the temporal points are $t^n = t^0 + nk$, $t^0 = 0.5$, $0 \le n \le N = 10000$, in the temporal domain $[0, \tau = 5.5]$. Plot (a): Successive absolute differences for the mean of the approximate melting interface s.p.: $\text{AbsDiff}\left[\mu\left(s_{K_\ell, K_{\ell+1}}(t^n, \omega)\right)\right]$ Plot (b): Successive absolute differences for the standard deviation of the approximate melting interface s.p.: $\text{AbsDiff}\left[\sigma\left(s_{K_\ell, K_{\ell+1}}(t^n, \omega)\right)\right]$.

Table 2
Maximum values of the absolute differences for both statistical moments (42) between two successive realizations $\{K_\ell, K_{\ell+1}\}$, $K_\ell \in \{10, 20, 40, 80, 160\}$, of the approximate temperature s.p. after $\tau = 5.5$ min. Both step-sizes are considered fixed $(h, k) = (0.1, 5e-04)$. The spatial points generated are $z_i = ih$, $1 \le i \le M - 1 = 10$.

$\{K_\ell, K_{\ell+1}\}$	$\left\|\text{AbsDiff}\left[\mu\left(u_{K_\ell K_{\ell+1}}(z_i, \tau, \omega)\right)\right]\right\|_\infty$ °C	$\left\|\text{AbsDiff}\left[\sigma\left(u_{K_\ell K_{\ell+1}}(z_i, \tau, \omega)\right)\right]\right\|_\infty$ °C
{10, 20}	6.0329e − 04	4.2305e − 04
{20, 40}	1.8666e − 04	4.4532e − 04
{40, 80}	8.4877e − 05	2.0694e − 04
{80, 160}	2.2298e − 05	1.0487e − 04

Table 3
Maximum values of the absolute differences for both statistical moments (43) between two successive realizations $\{K_\ell, K_{\ell+1}\}$, $K_\ell \in \{10, 20, 40, 80, 160\}$, of the approximate melting interface from 0 up to $\tau = 5.5$ min. Both step-sizes are considered fixed $(h, k) = (0.1, 5e-04)$. The temporal points generated are $t^n = t^0 + nk$, $t^0 = 0.5$, $0 \le n \le N = 10000$.

$\{K_\ell, K_{\ell+1}\}$	$\left\|\text{AbsDiff}\left[\mu\left(s_{K_\ell K_{\ell+1}}(t^n, \omega)\right)\right]\right\|_\infty$ mm	$\left\|\text{AbsDiff}\left[\sigma\left(s_{K_\ell K_{\ell+1}}(t^n, \omega)\right)\right]\right\|_\infty$ mm
{10, 20}	7.8291e − 02	1.0924e − 02
{20, 40}	2.8463e − 02	2.5850e − 03
{40, 80}	2.0654e − 02	3.5081e − 03
{80, 160}	1.8702e − 02	1.3207e − 03

$K = 80$ Monte Carlo realizations and the data of this Section 2.1 the stability of the approximations is guaranteed for a temporal step-size $k < 2\,\beta_{\min}^2\,t^0\,h^2 = 2\,(0.2399)^2\,0.5\,(0.025)^2 = 3.597\text{e}-05$ but not for the value $k = 6e-05$, for example, as Fig. 6 illustrates.

Once we have seen the reliability of the computed approximations for both statistical moments of the temperature s.p and the interface s.p. even for a few Monte Carlo realizations (for example $K = 80$ realizations, see Tables 2–3), we illustrate in Fig. 7 the evolution of the approximations to the mean of the temperature s.p. for several temporal instants $\tau = \{1.5, 2.5, 3.5, 4.5, 5.5\}$ minutes. We observe that the mean of the temperature s.p. follows a decreasing behaviour in the spatial variable from the left hot end condition fixed at 10 °C to the interface value at 0 °C. The red large points in the abscissae represent where the mean of the melting interface is placed at each time τ. The melting interface is moving towards the right because the ice block is melting along the time. In the bottom right

Table 4
CPU time seconds and their corresponding real time in seconds spent to compute both statistical moments at $\tau = 5.5$ min with the fixed step-sizes $(h, k) = (0.1, 5e-04)$ while the number of Monte Carlo realizations, K, varies.

K	$[\mu/\sigma]\ (u_K(z_i,\tau,\omega), s_k(t^n,\omega))$ CPU, s	$[\mu/\sigma]\ (u_K(z_i,\tau,\omega), s_k(t^n,\omega))$ real time (s)
10	0.8281	0.36
20	0.9688	0.27
40	1.5156	0.34
80	1.9688	0.60
160	1.8594	1.12

Table 5
Maximum values of the absolute errors for both statistical moments (44) of the approximate temperature s.p. after $\tau = 1$ min. The step-sizes (h, k) are refined while the number of the Monte Carlo realizations is the fixed value $K = 500$. The values M and N are the spatial and temporal levels, respectively.

(h, k)	(M, N)	$\|\text{AbsErr}\,[\mu\,(u_K(z_i,\tau,\omega))]\|_\infty$ °C	$\|\text{AbsErr}\,[\sigma\,(u_K(z_i,\tau,\omega))]\|_\infty$ °C
(0.2, 2e − 03)	(5, 250)	1.8868e − 04	5.5296e − 05
(0.1, 5e − 04)	(10, 1000)	7.9923e − 05	6.1638e − 05
(0.05, 1e − 04)	(20, 50000)	5.3438e − 05	6.3238e − 05
(0.025, 3.5e − 05)	(40, 14286)	4.6993e − 05	6.3756e − 05

Table 6
Maximum values of the absolute errors for both statistical moments (44) of the approximate melting interface from 0 up to $\tau = 1$ min taking $t^0 = 0.5$. The step-sizes (h, k) are refined while the number of the Monte Carlo realizations is the fixed value $K = 500$. The values M and N are the spatial and temporal levels, respectively.

(h, k)	(M, N)	$\|\text{AbsErr}\,[\mu\,(s_K(t^n,\omega))]\|_\infty$ mm	$\|\text{AbsErr}\,[\sigma\,(s_K(t^n,\omega))]\|_\infty$ mm
(0.2, 2e − 03)	(5, 250)	6.2576e − 03	1.0473e − 03
(0.1, 5e − 04)	(10, 1000)	5.6742e − 03	1.0784e − 03
(0.05, 1e − 04)	(20, 50000)	5.5284e − 03	1.0861e − 03
(0.025, 3.5e − 05)	(40, 14286)	5.4967e − 03	1.0878e − 03

Table 7
CPU time seconds and their corresponding real time in seconds spent to compute both statistical moments at $\tau = 1$ min with a fixed number of Monte Carlo realizations $K = 500$ while step-sizes (h, k) vary.

(h, k)	$[\mu/\sigma]\ (u_K(z_i,\tau,\omega), s_K(t^n,\omega))$ CPU, s	$[\mu/\sigma]\ (u_K(z_i,\tau,\omega), s_K(t^n,\omega))$ real time (s)
(0.2, 2e − 03)	0.9375	0.38
(0.1, 5e − 04)	2.2813	1.50
(0.05, 1e − 04)	9.4844	7.84
(0.025, 3.5e − 05)	37.2813	33.37

of Fig. 7 we show the complete evolution of the mean for the melting interface throughout the 5.5 min and in the bottom left we plot its standard deviation. Fig. 8 shows the evolution of the approximations to the standard deviation of the temperature s.p. for several temporal instants $\tau = \{1.5, 2.5, 3.5, 4.5, 5.5\}$ minutes.

3. Random binary metallic alloys

We consider the finite domain $\mathcal{D} = [0, \ell]$ that is, composed by a particle in the spatial domain $[0, s(t,\omega))$ and a diffusive phase $(s(t,\omega), \ell]$ being $s(t,\omega)$ the interface s.p. The concentration $C(x,t,\omega)$ of the material follows the random Stefan model (9)–(13) under conditions (1)–(2). Firstly, we use a random front-fixing transformation of

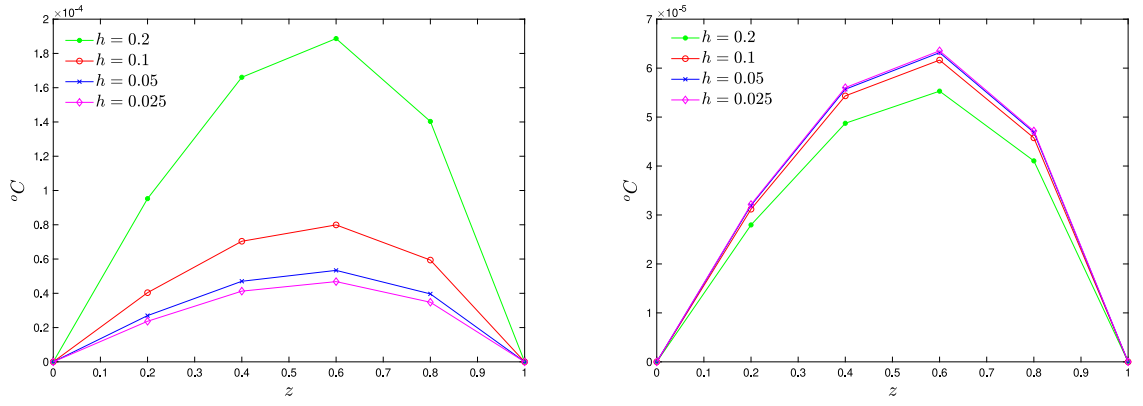

(a) (b)

Fig. 4. Absolute errors after $\tau = 1$ min for both statistical moments of the approximate temperature s.p., $u_K(z, \tau, \omega)$, computed by (44) for $K = 500$ Monte Carlo simulations and considering several step-sizes $(h, k) \in \{(0.2, 2e-03), (0.1, 5e-04), (0.05, 1e-04), (0.025, 3.5e-05)\}$. Plot (a): Absolute error of the mean of the approximate temperature s.p.: AbsErr $[\mu\,(u_K\,(z, 1, \omega))]$. Plot (b): Absolute errors for the standard deviation of the approximate temperature s.p.: AbsErr $[\sigma\,(u_K\,(z, 1, \omega))]$.

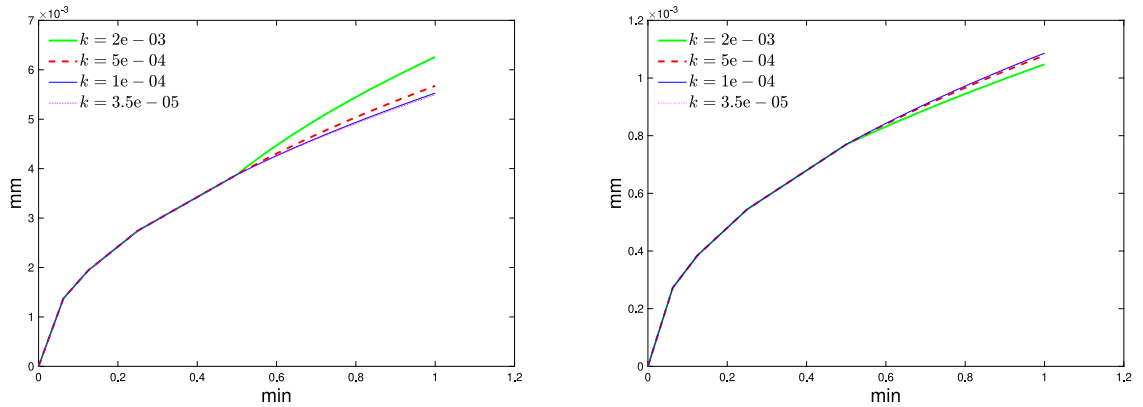

(a) (b)

Fig. 5. Absolute errors over $\tau = 1$ min for both statistical moments of the approximate melting interface s.p. computed by (44) for $K = 500$ Monte Carlo simulations and considering several step-sizes $(h, k) \in \{(0.2, 2e-03), (0.1, 5e-04), (0.05, 1e-04), (0.025, 3.5e-05)\}$. Plot (a): Absolute error of the mean of the approximate interface s.p.: AbsErr $[\mu\,(s_K\,(t^n, \omega))]$. Plot (b): Absolute errors for the standard deviation of the approximate interface s.p.: AbsErr $[\sigma\,(s_K\,(t^n, \omega))]$.

Landau type for immobilizating the diffusive phase domain $(s(t, \omega), \ell]$

$$z = \frac{\ell - x(t, \omega)}{\ell - s(t, \omega)}, \quad \omega \in \Omega, \ t > 0, \tag{45}$$

where z is a real variable in the interval $[0, 1]$. Note that the point $z = 0$ corresponds to the right end of the domain ℓ and $z = 1$ represents the left end of the diffusive phase domain $s(t, \omega)$. The transformed dependent variable denoted by

$$v(z, t, \omega) = C(x(t, \omega), t, \omega), \quad \omega \in \Omega, \tag{46}$$

is the solution s.p. of the random transformed Stefan problem

$$\frac{\partial v(z, t, \omega)}{\partial t} = \frac{D(\omega)}{(\ell - s(t, \omega))^2} \frac{\partial^2 v(z, t, \omega)}{\partial z^2} + z \frac{s'(t, \omega)}{\ell - s(t, \omega)} \frac{\partial v(z, t, \omega)}{\partial z}, \quad 0 < z < 1, \quad t > 0, \quad \omega \in \Omega, \tag{47}$$

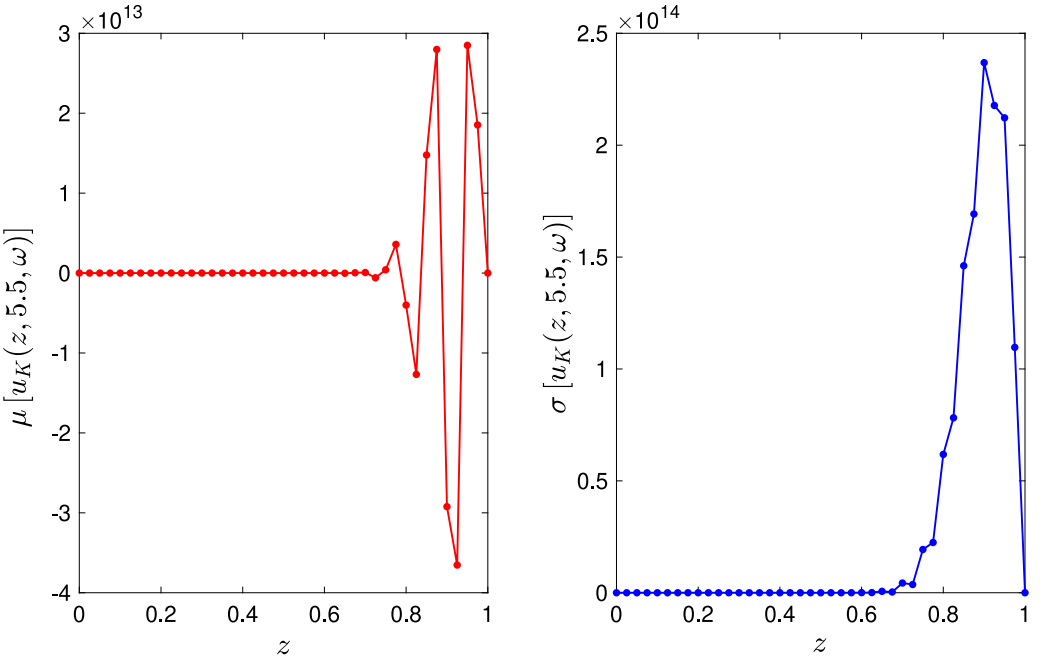

Fig. 6. Unstable approximations for both statistical moments of temperature s.p. after $\tau = 5.5$ min considering the temporal step-size $k = 6\mathrm{e}-05$ breaking the stability condition (40) taking $h = 0.025$, $t^0 = 0.5$ and $K = 80$ Monte Carlo realizations. Plot (a): Mean of the approximate temperature s.p. Plot (b): Standard deviation of the approximate temperature s.p.

with the boundary conditions

$$\left.\frac{\partial v(z,t,\omega)}{\partial z}\right|_{z\to 0^+} = 0\,,\ t>0\,,\quad \omega\in\Omega, \tag{48}$$

$$v(1,t,\omega) = c^{\mathrm{sol}}\,,\ t>0\,,\quad \omega\in\Omega, \tag{49}$$

and the transformed Stefan condition

$$(c^{\mathrm{part}}-c^{\mathrm{sol}})\,s'(t,\omega) = -\frac{D(\omega)}{\ell - s(t,\omega)}\left.\frac{\partial v(z,t,\omega)}{\partial z}\right|_{z\to 1^-},\ t>0,\quad \omega\in\Omega, \tag{50}$$

where $s'(t,\omega)$ denotes the first mean square derivative $\frac{\mathrm{d}s(t,\omega)}{\mathrm{d}t}$, $\omega\in\Omega$.

Remark 2. In order to legitimate the mean square operational calculus developed in (47) and (50) it is important to point out that

$$\frac{\partial^2 v(z,t,\cdot)}{\partial z^2}\,,\quad \frac{\partial v(z,t,\cdot)}{\partial z}\,,\quad \frac{\partial v(z,t,\cdot)}{\partial t}\,,\quad \frac{s'(t,\cdot)}{\ell - s(t,\cdot)}\,,\quad \frac{1}{\ell - s(t,\cdot)}\,,\quad \frac{1}{(\ell - s(t,\cdot))^2} \tag{51}$$

lie in $L_4(\Omega)$, see [23, Sec. 3].

The random transformed initial condition is taken in a small $t^0 > 0$ and not in $t = 0$, in order to preserve the behaviour of the exact solutions of the concentration and the interface in a semi-infinite domain for the deterministic case for $0 < t \le t^0$, see [9],

$$c(x,t) = \begin{cases} c^{\mathrm{part}}\,, & 0\le x\le s(t)\,,\\[2ex] c^0 + \dfrac{\left(c^{\mathrm{sol}}-c^0\right)\operatorname{erfc}\left(\frac{x-b_0}{2\sqrt{Dt}}\right)}{\operatorname{erfc}\left(\frac{\alpha}{\sqrt{D}}\right)}\,, & x\ge s(t)\,, \end{cases} \tag{52}$$

$$s(t) = b_0 + 2\,\alpha\,\sqrt{t}\,, \tag{53}$$

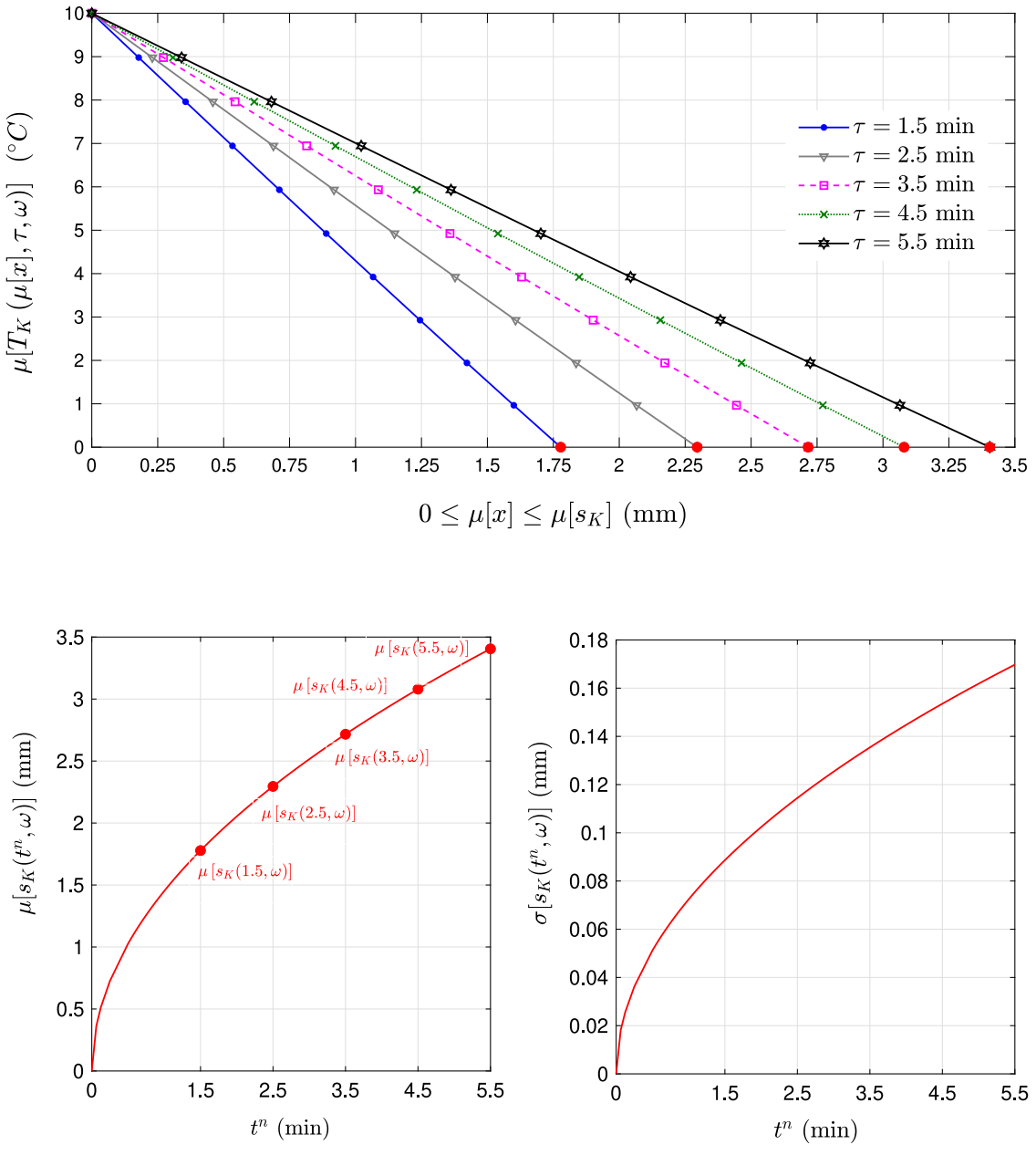

Fig. 7. Evolution of the approximations of the mean of the temperature s.p. $\mu[T_K(\mu[x],\tau,\omega)]$ at several temporal instants $\tau = \{1.5, 2.5, 3.5, 4.5, 5.5\}$ min for the step-sizes ($h = 0.1, k = 5\text{e}-04$) and $K = 80$ Monte Carlo realizations. (Bottom left plot) Evolution of the mean for the melting interface $\mu[s_K(t^n,\omega)]$ up to 5.5 min. (Bottom right plot) Evolution of the standard deviation for the melting interface $\sigma[s_K(t^n,\omega)]$ up to 5.5 min.

where α is the root of the non-linear algebraic equation

$$\alpha = \frac{c^0 - c^{\text{sol}}}{c^{\text{part}} - c^{\text{sol}}} \sqrt{\frac{D}{\pi}} \frac{\text{e}^{\frac{-\alpha^2}{D}}}{\text{erfc}\left(\frac{\alpha}{\sqrt{D}}\right)}. \tag{54}$$

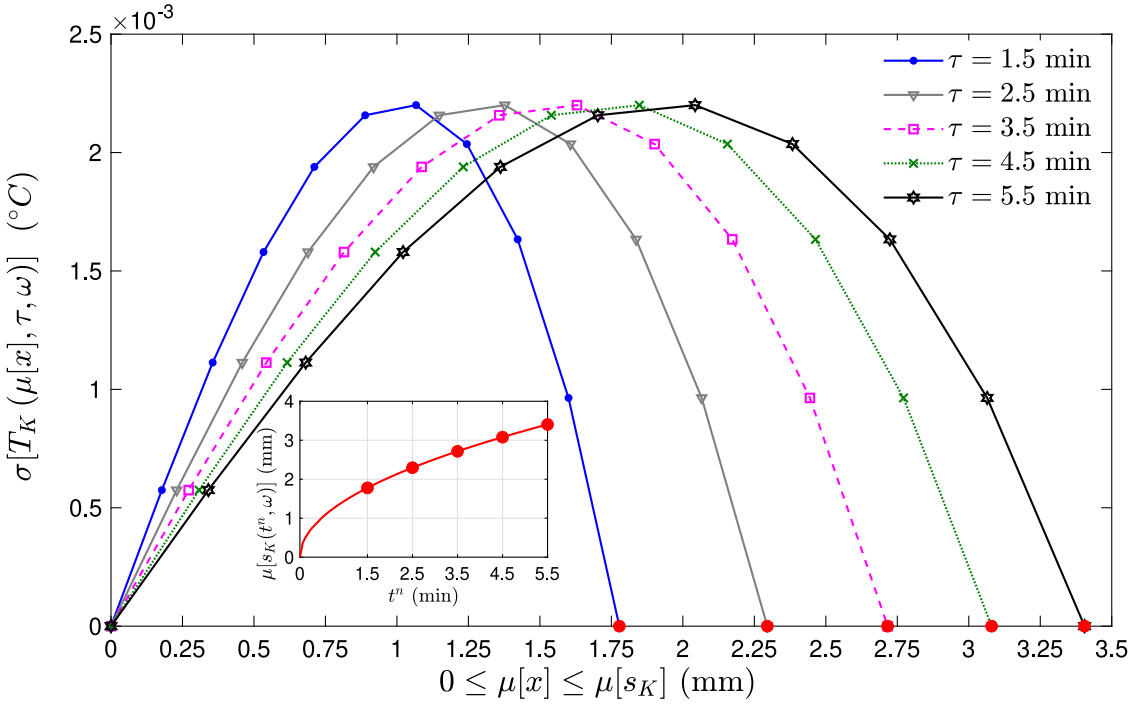

Fig. 8. Evolution of the approximations of the standard deviation of the temperature s.p. $\sigma\left[T_K\left(\mu[x],\tau,\omega\right)\right]$ at several temporal instants $\tau = \{1.5, 2.5, 3.5, 4.5, 5.5\}$ min considering $K = 80$ Monte Carlo realizations and the step-sizes ($h = 0.1, k = 5\mathrm{e}-04$). The red large points in the abscissae indicate where the mean of the interface s.p. $\sigma\left[s_K\left(t^n,\omega\right)\right]$ is placed which moves with the time t^n, $0 \le t^n \le 5.5$ min.

Hence, the random transformed front-fixing problem (47)–(50) is considered for $t > t^0$ instead of $t > 0$ with the initial conditions given by

$$v(z,t^0,\omega) = \begin{cases} c^0 + \dfrac{c^{\mathrm{sol}}-c^0}{\mathrm{erfc}\left(\frac{\alpha(\omega)}{\sqrt{D(\omega)}}\right)}\,\mathrm{erfc}\left(\dfrac{\ell-\left(\ell-b_0-2\,\alpha(\omega)\sqrt{t^0}\right)z-b_0}{2\sqrt{D(\omega)\,t^0}}\right), & 0 \le z \le 1\,, \\ c^{\mathrm{part}}\,, & 1 < z < \dfrac{\ell}{\ell-s(t^0,\omega)}\,, \end{cases} \tag{55}$$

$$s(t^0,\omega) = b_0 + 2\,\alpha(\omega)\,\sqrt{t^0}\,, \tag{56}$$

where the r.v. $\alpha(\omega)$ is the solution of the random non-linear equation

$$\alpha(\omega) = \frac{c^0 - c^{\mathrm{sol}}}{c^{\mathrm{part}} - c^{\mathrm{sol}}}\sqrt{\frac{D(\omega)}{\pi}}\,\frac{\mathrm{e}^{\frac{-\alpha(\omega)^2}{D(\omega)}}}{\mathrm{erfc}\left(\frac{\alpha(\omega)}{\sqrt{D(\omega)}}\right)}. \tag{57}$$

Using the random difference method described in Section 2 and denoting the spatial mesh points $z_i = ih$, $0 \le i \le M$, such that $Mh = 1$ and time levels $t^n = nk + t^0$, $0 \le n \le N$ with $\tau = Nk + t^0$, we obtain the following

random explicit difference scheme for a small $t^0 > 0$

$$\left.\begin{array}{l} v_i^{n+1}(\omega) = a_i^n(\omega)\, v_{i-1}^n(\omega) + b^n(\omega)\, v_i^n(\omega) + c_i^n(\omega)\, v_{i+1}^n\,, \quad \omega \in \Omega\,, \\ \qquad\qquad\qquad\qquad\qquad\qquad\qquad\qquad 1 \le i \le M-1,\ 0 \le n \le N-1\,, \\ v_0^n(\omega) = \dfrac{4v_1^n - v_2^n}{3}\,, \quad v_M^n(\omega) = c^{\rm sol}\,, \quad 0 \le n \le N\,, \\ v_i^0(\omega) = c^0 + \dfrac{c^{\rm sol} - c^0}{\operatorname{erfc}\left(\frac{\alpha(\omega)}{\sqrt{D(\omega)}}\right)} \operatorname{erfc}\left(\dfrac{\ell - \left(\ell - b_0 - 2\,\alpha(\omega)\sqrt{t^0}\right) z_i - b_0}{2\sqrt{D(\omega)\, t^0}}\right)\,, \quad 0 \le i \le M\,. \end{array}\right\} \tag{58}$$

with the random coefficients

$$\left.\begin{array}{l} a_i^n(\omega) = \dfrac{k\, D(\omega)}{h^2(\ell - s^n(\omega))^2}\left(1 + \dfrac{\Delta^n(\omega)}{4(c^{\rm part} - c^{\rm sol})} z_i\right) \\ b^n(\omega) = 1 - \dfrac{2kD(\omega)}{h^2\,(\ell - s^n(\omega))^2} \\ c_i^n(\omega) = \dfrac{k\, D(\omega)}{h^2(\ell - s^n(\omega))^2}\left(1 - \dfrac{\Delta^n(\omega)}{4(c^{\rm part} - c^{\rm sol})} z_i\right) \end{array}\right\} \quad 1 \le i \le M-1, \quad 0 \le n \le N-1\,,\ \omega \in \Omega\,, \tag{59}$$

where the discretized approximations of the s.p.'s $v(z_i, t^n, \omega)$ and $s(t^n, \omega)$ are denoted by $v_i^n(\omega)$ and $s^n(\omega)$ respectively. In (59) $\Delta^n(\omega)$ is given by

$$\Delta^n(\omega) = 3v_M^n(\omega) - 4v_{M-1}^n(\omega) + v_{M-2}^n(\omega) \approx 2h\left(\left.\frac{\partial v(z, t^n, \omega)}{\partial z}\right|_{z \to 1^-}\right). \tag{60}$$

Next technical result shows the negativity of $\Delta^n(\omega)$, $\omega \in \Omega$, for every time level n.

Lemma 1. *For each realization $\omega_l \in \Omega$, the terms $\Delta^n(\omega_l)$ defined by (60) are negative for $0 \le n \le N$.*

Proof. For $n = 0$, it is verified $\Delta^0(\omega_l) \approx 2h\left(\left.\frac{\partial v(z, t^0, \omega_l)}{\partial z}\right|_{z \to 1^-}\right) < 0$ due to the fact that the sampling random function $v(z, t^0, \omega_l)$ given by (55) is decreasing differentiable function in z. For induction hypothesis, we assume

$$\Delta^n(\omega_l) < 0, \quad 0 \le n \le N-1,\ \omega_l \in \Omega\ . \tag{61}$$

Consider the Taylor expansion of $\Delta^{n+1}(\omega_l)$ at t^n up to first order

$$\Delta^{n+1}(\omega_l) = \Delta^n(\omega_l) + \ \mathrm{O}(k)\,, \quad 0 \le n \le N-1\,,\ \omega_l \in \Omega.$$

Then for a small enough temporal step-size k one gets

$$\Delta^{n+1}(\omega_l) < 0, \quad 0 \le n \le N-1\,,\ \omega_l \in \Omega.$$

The random difference scheme for the interface s.p. takes the form

$$\left.\begin{array}{rcl} s^{n+1}(\omega) & = & s^n(\omega) - \dfrac{k\ D(\omega)\ \Delta^n(\omega)}{(c^{\rm part} - c^{\rm sol})(\ell - s^n(\omega))\, 2h}\,, \quad 0 \le n \le N-1\,, \\ s^0(\omega) & = & b_0 + 2\,\alpha(\omega)\sqrt{t^0}\,, \quad t^0 > 0\,, \end{array}\right\}\,,\ \omega \in \Omega\,. \tag{62}$$

The numerical analysis of the random schemes (58)–(62) is treated in the next Section 3.1 paying special attention to the positivity, monotonicity and stability in the mean square sense.

3.1. Qualitative properties of the numerical solution s.p.'s

Dealing with concentrations the positivity of the solution is a property that must be guaranteed. With respect to the monotonicity of its random scheme let us introduce the following definition

Definition 1. We say that the random numerical solution $\{v_i^n(\omega)\}$, $\omega \in \Omega$ of a random finite difference scheme is a decreasing monotone one in the spatial index $i \in I$, if it holds

$$v_i^n(\omega_l) > v_{i+1}^n(\omega_l)\,,$$

for every realization $\omega_l \in \Omega$ with $i, i+1 \in I$.

For the sake of clarity in the presentation let us recall the definition of $\|\cdot\|_p$ stability of a random finite scheme, see [5].

Definition 2. A random numerical scheme is said to be $\|\cdot\|_p$-stable in the fixed station sense in the domain $[0,1] \times [t^0, \tau]$, if for every partition with $k = \Delta t$, $h = \Delta x$ such that $t^0 + N k = \tau$ and $M h = 1$,

$$\|v_i^n\|_p \le R\,, \quad 0 \le i \le M, \quad 0 \le n \le N\,, \tag{63}$$

where R is independent of the step-sizes h, k and the time level n.

Consider the deterministic sampling schemes corresponding to the random schemes (58)–(62) by fixing a realization $\omega_l \in \Omega$. Starting with a positive initial condition in (55) note that the positivity of the sampling coefficients $a_i^n(\omega_l)$, $b^n(\omega_l)$ and $c_i^n(\omega_l)$ in (59) is a sufficient condition for the positivity of the numerical sample solution $v_i^n(\omega_l)$. Note that $\Delta^n(\omega_l) = O(h)$ from (60), then the coefficients $a_i^n(\omega_l)$ and $c_i^n(\omega_l)$ are positive for a small enough spatial step-size h. The study of the sign of coefficients $b^n(\omega_l)$ is based in the following remark.

Remark 3. We can obtain an upper bound of the interface along the time by means a balance of mass. On the one hand, the total initial mass is $c^{\text{part}} b_0 + c^0(\ell - b_0)$ from (11). On the other hand, in the final steady state the position of the interface, s_∞, does not move and the concentration of all the diffusive part remains constant with value c^{sol}. Thus using the balance of mass argument and noting that $b_0 < \ell$ one gets

$$s_\infty = \frac{(c^{\text{part}} - c^0) b_0 + (c^0 - c^{\text{sol}})\ell}{c^{\text{part}} - c^{\text{sol}}} \le \delta_S < \ell\,, \tag{64}$$

where δ_s is an upper bound of the final steady position of the interface, s_∞, being lower than ℓ. Attending the result proved in Lemma 1 and using the sampling random scheme (62) for the interface s.p. it is guaranteed the increasing behaviour of the interface s.p. along the time for each realization $\omega_l \in \Omega$

$$s^{n+1}(\omega_l) > s^n(\omega_l)\,, \quad \omega_l \in \Omega\,, \quad 0 \le n \le N-1\,. \tag{65}$$

Moreover, the interface at each time level n is bounded as

$$s^n(\omega_l) < s_\infty \le \delta_S < \ell, \quad 0 \le n \le N\,, \quad \omega_l \in \Omega\,. \tag{66}$$

Under the property (66) and from (59) it follows that

$$b^n(\omega_l) = 1 - \frac{2k D(\omega_l)}{h^2(\ell - s^n(\omega_l))^2} > 1 - \frac{2k D(\omega_l)}{h^2(\ell - \delta_s)^2}, \quad 0 \le n \le N-1\,.$$

Then under condition

$$\frac{k}{h^2} < \frac{(\ell - \delta_s)^2}{2\max\{D(\omega) : \omega \in \Omega\}}, \tag{67}$$

the positivity of coefficient $b^n(\omega_l)$ is guaranteed.

Let us now check the decreasing monotonicity of the sampling numerical solution $\{v_i^n(\omega_l)\}$ in the spatial index i for every time level n. In fact, for $n = 0$ the sampling random function $v(z, t^0, \omega_l)$ given by (55) is decreasing differentiable function in z. For induction hypothesis, we assume

$$v_i^n(\omega_l) > v_{i+1}^n(\omega_l), \quad 0 \le i \le M-1,\ \omega_l \in \Omega\ . \tag{68}$$

Then using (68) one gets

$$\begin{aligned} v_{i+1}^{n+1}(\omega_l) &= a_{i+1}^n(\omega_l)\, v_i^n(\omega_l) + b^n(\omega_l)\, v_{i+1}^n(\omega_l) + c_{i+1}^n(\omega_l)\, v_{i+2}^n(\omega_l) \\ &< a_{i+1}^n(\omega_l)\, v_i^n(\omega_l) + b^n(\omega_l)\, v_{i+1}^n(\omega_l) + c_{i+1}^n(\omega_l)\, v_{i+1}^n(\omega_l)\,, \quad 0 \le i \le M-2\,, \end{aligned} \tag{69}$$

$$v_i^{n+1}(\omega_l) = a_i^n(\omega_l)\, v_{i-1}^n(\omega_l) + b^n(\omega_l)\, v_i^n(\omega_l) + c_i^n(\omega_l)\, v_{i+1}^n(\omega_l)$$
$$> a_i^n(\omega_l)\, v_i^n(\omega_l) + b^n(\omega_l)\, v_i^n(\omega_l) + c_i^n(\omega_l)\, v_{i+1}^n(\omega_l)\,, \quad 1 \le i \le M-1\,. \tag{70}$$

Subtracting expressions (69)–(70) it follows that

$$\begin{aligned} & v_{i+1}^{n+1}(\omega_l) - v_i^{n+1}(\omega_l) \\ & < \left(a_{i+1}^n(\omega_l) - a_i^n(\omega_l) - b^n(\omega_l)\right) v_i^n(\omega_l) + \left(b^n(\omega_l) + c_{i+1}^n(\omega_l) - c_i^n(\omega_l)\right) v_{i+1}^n(\omega_l) \\ & = \left(\frac{k}{h^2(\ell - s^n(\omega_l))^2}\,\frac{D(\omega_l)\Delta^n(\omega_l)(z_{i+1}-z_i)}{4(c^{\text{part}}-c^{\text{sol}})} - 1 + \frac{2kD(\omega_l)}{h^2(\ell - s^n(\omega_l))^2}\right) v_i^n(\omega_l) + \\ & \left(1 - \frac{2kD(\omega_l)}{h^2(\ell - s^n(\omega_l))^2} - \frac{k}{h^2(\ell - s^n(\omega_l))^2}\,\frac{D(\omega_l)\Delta^n(\omega_l)(z_{i+1}-z_i)}{4(c^{\text{part}}-c^{\text{sol}})}\right) v_{i+1}^n(\omega_l) \\ & = \left(1 - \frac{2kD(\omega_l)}{h^2(\ell - s^n(\omega_l))^2}\left(1 + \frac{h\Delta^n(\omega_l)}{8(c^{\text{part}}-c^{\text{sol}})}\right)\right)\left(v_{i+1}^n(\omega_l) - v_i^n(\omega_l)\right)\,, \quad 1 \le i \le M-2\,. \end{aligned} \tag{71}$$

From (71) using Lemma 1 and condition (67) one gets

$$v_i^{n+1}(\omega_l) > v_{i+1}^{n+1}(\omega_l)\,, \quad 0 \le i \le M-1,\ \omega_l \in \Omega\ .$$

Finally, it is necessary to prove that the sampling random solution $\{v_i^n(\omega_l)\}$ is decreasing in the endpoints. In fact, note that $a_i^n(\omega_l) + b^n(\omega_l) + c_i^n(\omega_l) = 1$, see (59), then taking the sampling numerical scheme (58) for $j = M-1$ and the induction hypothesis (68)

$$v_{M-1}^{n+1}(\omega_l) > \left(a_{M-1}^n(\omega_l) + b^n(\omega_l) + c_{M-1}^n(\omega_l)\right) v_M^n(\omega_l) = c^{\text{part}} = u_M^{n+1}(\omega_l)\,.$$

In the other endpoint, using the boundary condition appearing in (58) and the decreasing behaviour in the internal points we also obtain the decreasing of sampling numerical solution

$$v_0^{n+1}(\omega_l) = \frac{1}{3}\left(4v_1^{n+1}(\omega_l) - v_2^{n+1}(\omega_l)\right) = \frac{1}{3}\left(3v_1^{n+1}(\omega_l) + v_1^{n+1}(\omega_l) - v_2^{n+1}(\omega_l)\right) > v_1^{n+1}(\omega_l)\,.$$

Dealing with the $\|\cdot\|_p$-stability in the fixed station sense, see Definition 2, and taking into account the decreasing monotonicity of $\{v_i^n(\omega_l)\}$, it is relevant to study the boundedness of $v_0^n(\omega_l)$, $\omega_l \in \Omega$, $0 \le n \le N$. In fact, $v_0^0(\omega_l) < c^0$ for (58). Furthermore, $v_0^n(\omega_l) = v_1^n(\omega_l) + \mathrm{O}(h)$ and using an induction hypothesis one gets

$$v_1^{n+1}(\omega_l) < (a_1^n(\omega_l) + b^n(\omega_l) + c_1^n(\omega_l))v_0^n(\omega_l) = v_0^n(\omega_l) < c^0.$$

Then $v_0^{n+1}(\omega_l) = v_1^{n+1}(\omega_l) + \mathrm{O}(h) < c^0$ for small enough h. Using that the sequence $\{v_i^n(\omega_l)\}$ decreases in the spatial index i we conclude

$$v_i^n(\omega_l) < c^0, \quad 0 \le n \le N,\ 0 \le i \le M,\ \omega_l \in \Omega. \tag{72}$$

As a result the $\|\cdot\|_p$ of the random numerical solution $\{v_i^n(\omega)\}$ satisfies

$$\|v_i^n\|_p = \left(\mathbb{E}\left[\left|v_i^n\right|^p\right]\right)^{1/p} = \left(\int_\Omega \left|v_i^n(\omega)\right|^p f_{v_i^n}(\omega)\,\mathrm{d}\omega\right)^{1/p} \le c^0 \underbrace{\left(\int_\Omega f_{v_i^n}(\omega)\,\mathrm{d}\omega\right)^{1/p}}_{1}, \tag{73}$$

where $f_{v_i^n}$ is the density function of the r.v. v_i^n.

The next theorem summarizes the results proved above.

Theorem 1. *With the previous notation for small enough values of the discretization step-sizes $h = \Delta z$ and $k = \Delta t$ verifying the condition (67) the random numerical finite difference solution $\{v_i^n(\omega)\}$, $\omega \in \Omega$ given by (58)–(59) for the concentration of the diffusive part satisfies*

(i) $\{v_i^n(\omega)\}$ is positive for $0 \le i \le M$ at each time-level $0 \le n \le N$ with $\tau = t^0 + Nk$, $t^0 > 0$.
(ii) $\{v_i^n(\omega)\}$ is a monotonically decreasing sequence in the spatial index i for each time level n.
(iii) $\{v_i^n(\omega)\}$ is $\|\cdot\|_p$-stable in the fixed station sense.

Moreover, the random numerical solution (62) $s^n(\omega)$, $0 \le n \le N$, $\omega \in \Omega$, of the interface s.p. increases along the time and its boundedness is given by (66).

Table 8
Maximum values of the absolute deviations (74) varying the simulations $K \in \{25, 50, 100, 200, 400, 800\}$ for both statistical moments of the random numerical concentration, $v_{K_\ell}(z_i, \tau, \omega)$, at the final time instant $\tau = 1 = t^0 + Nk$, $t^0 = 0.01$, $k = 4\text{e}-04$ ($N = 2475$), in the spatial points $z_i = ih$, $1 \le i \le M - 1 = 19$, $h = 0.05$.

$\{K_\ell, K_{\ell+1}\}$	$\left\|\text{AbsDev}\left[\mu\left(v_{K_\ell K_{\ell+1}}(z_i,\tau,\omega)\right)\right]\right\|_\infty$	$\left\|\text{AbsDev}\left[\sigma\left(v_{K_\ell K_{\ell+1}}(z_i,\tau,\omega)\right)\right]\right\|_\infty$
{25, 50}	1.0667e − 04	4.0336e − 05
{50, 100}	7.8659e − 05	1.8529e − 05
{100, 200}	3.6368e − 05	3.1843e − 05
{200, 400}	4.8083e − 05	8.3587e − 06
{400, 800}	7.9087e − 06	3.4383e − 06

3.2. Example

In this example we illustrate the results of this section considering some deterministic data used in [9, Sec. 4]. In particular, we take the initial condition of the concentration $C(x, 0)$ in (11) with $c^{\text{part}} = 0.53$, $c^{\text{sol}} = 0$, $c^0 = 0.1$ verifying the relationship ($c^{\text{part}} > c^0 > c^{\text{sol}} > 0$), $\ell = 1$ and $b_0 = 0.2$. We choose the r.v. $D(\omega)$ following a normal distribution of mean 1 and standard deviation 0.1 truncated in the interval [0.8, 1.2], that is, $N_{[0.8,1.2]}(1, 0.1)$. In order to initialize the deterministic sampling schemes corresponding to the random schemes (58)–(60) by fixing a realization $\omega_l \in \Omega$ we take $t^0 = 0.01$. For $0 < t \le t^0$, we use the exact solution given by (52)–(54). As the exact solution is not available at $t > t^0$ we study the numerical convergence using a Cauchy type condition varying the number K of realizations as well as the step-sizes of discretization (h, k). With the spatial step-size h chosen the election of the temporal step-size k can be done using the sufficient $\|\cdot\|_p$-stability condition (67) taking $\delta_s = 0.36$ computed by (66) and $\max\{D(\omega) : \omega \in \Omega\} = 1.2$.

For the first study, we use the following notation related to the numerical means and standard deviations

$$\begin{aligned}
\text{AbsDev}\left[\mu\left(v_{K_\ell K_{\ell+1}}(z_i,\tau,\omega)\right)\right] &= \left|\mu\left(v_{K_{\ell+1}}(z_i,\tau,\omega)\right) - \mu\left(v_{K_\ell}(z_i,\tau,\omega)\right)\right|, \quad \omega \in \Omega,\\
\text{AbsDev}\left[\sigma\left(v_{K_\ell K_{\ell+1}}(z_i,\tau,\omega)\right)\right] &= \left|\sigma\left(v_{K_{\ell+1}}(z_i,\tau,\omega)\right) - \sigma\left(v_{K_\ell}(z_i,\tau,\omega)\right)\right|, \quad \omega \in \Omega.
\end{aligned} \tag{74}$$

$$\begin{aligned}
\text{AbsDev}\left[\mu\left(s_{K_\ell K_{\ell+1}}(t^n,\omega)\right)\right] &= \left|\mu\left(s_{K_{\ell+1}}(t^n,\omega)\right) - \mu\left(s_{K_\ell}(t^n,\omega)\right)\right|, \quad \omega \in \Omega,\\
\text{AbsDev}\left[\sigma\left(s_{K_\ell K_{\ell+1}}(t^n,\omega)\right)\right] &= \left|\sigma\left(s_{K_{\ell+1}}(t^n,\omega)\right) - \sigma\left(s_{K_\ell}(t^n,\omega)\right)\right|, \quad \omega \in \Omega.
\end{aligned} \tag{75}$$

where K_ℓ and $K_{\ell+1}$ are two successive numbers of realizations, $\tau = t^0 + Nk$ and $t^n = t^0 + nk$. Table 8 and Table 9 collect the values of the infinite norm of the successive absolute deviations (74)–(75) of the numerical concentration s.p. and the interface s.p., respectively, as the number of realizations increases for both statistical moments. Fig. 9 and Fig. 10 illustrate this decreasing behaviour for the successive absolute deviations (74)–(75).

For the second study we defined the following absolute deviations for a fixed number K of realizations whereas two successive step-sizes (h_ℓ, k_ℓ) and $(h_{\ell+1} = \frac{h_\ell}{2}, k_{\ell+1})$ vary verifying the stability condition (67)

$$\begin{aligned}
\text{AbsDev}\left[\mu\left(v_{K,h_\ell,h_{\ell+1}}(z_i,\tau,\omega)\right)\right] &= \left|\mu\left(v_{K,h_{\ell+1}}(z_i,\tau,\omega)\right) - \mu\left(v_{K,h_\ell}(z_i,\tau,\omega)\right)\right|, \quad \omega \in \Omega,\\
\text{AbsDev}\left[\sigma\left(v_{K,h_\ell,h_{\ell+1}}(z_i,\tau,\omega)\right)\right] &= \left|\sigma\left(v_{K,h_{\ell+1}}(z_i,\tau,\omega)\right) - \sigma\left(v_{K,h_\ell}(z_i,\tau,\omega)\right)\right|, \quad \omega \in \Omega.
\end{aligned} \tag{76}$$

The values described in (76) are collected in Table 10 for the infinite norm of the absolute deviations (76), it is observed that the proximity between successive approximations increases when the spatial step-sizes are refined for $K = 100$ realizations. Fig. 11 illustrates this trend between the approximations of the absolute deviations (76) over time $\tau = 1$. About the numerical interface s.p., in order to check that its mean has an upper bound $s_\infty = 0.3509$ along the time we compare in Table 11 their consecutive differences of both statistical moments (that is, μ-differences and σ-differences) as the time step-size k is refined in the last time instant $t^N = t^0 + Nk = 1$. Fig. 12 shows the evolution of both statistical moments of the interface s.p. along the time $\tau = 1$ for different values of time step-size k observing for the mean of the interface s.p. its asymptotic trend to s_∞ as the time step-size is refined considering only $K = 100$ realizations.

Table 12 collects these CPUs as well as the real time lapsed corresponding to these CPUs for the approximations of both statistical moments of the concentration s.p. and the interface s.p.

Due to the convergence of the approximations of both statistical moments of solutions s.p.'s is guaranteed, we show in Fig. 13 the evolution that the exact mean and standard deviation of the concentration s.p. describe in

Table 9
Maximum values of the absolute deviations (75) varying the simulations $K \in \{25, 50, 100, 200, 400, 800\}$ for both statistical moments of the random melting interface, $s_{K_\ell}(t^n, \omega)$, throughout the temporal levels $t^n = nk + t^0$, $t^0 = 0.01$, $1 \le n \le N$ with $k = 4\text{e}-04$ ($N = 2475$).

$\{K_\ell, K_{\ell+1}\}$	$\left\|\text{AbsDev}\left[\mu\left(s_{K_\ell K_{\ell+1}}(t^n,\omega)\right)\right]\right\|_\infty$	$\left\|\text{AbsDev}\left[\sigma\left(s_{K_\ell K_{\ell+1}}(t^n,\omega)\right)\right]\right\|_\infty$
{25, 50}	1.0566e − 03	6.7920e − 04
{50, 100}	9.5535e − 04	1.1640e − 04
{100, 200}	2.9821e − 04	2.9568e − 04
{200, 400}	5.9425e − 04	1.7460e − 04
{400, 800}	9.2035e − 05	2.1755e − 05

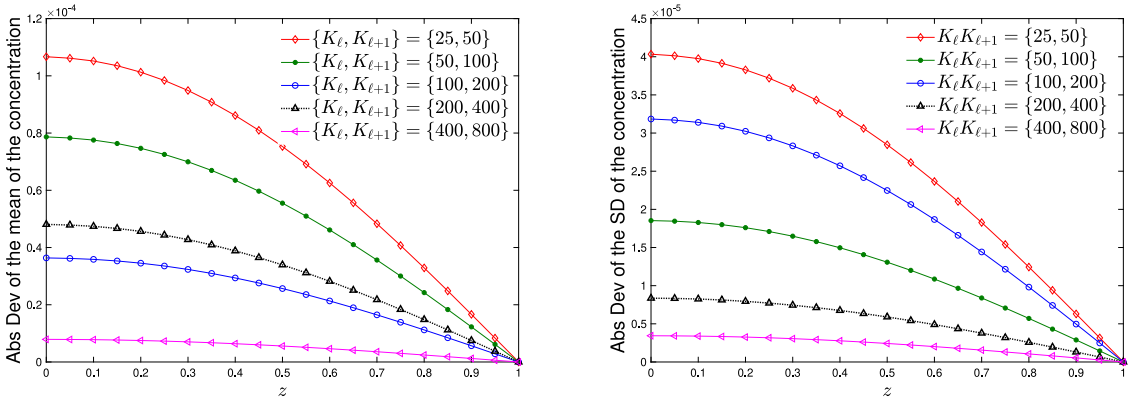

(a) (b)

Fig. 9. Absolute deviations over time $\tau = 1$ for both statistical moments of the approximate concentration s.p. between two successive realizations $\{K_\ell, K_{\ell+1}\}$, $K_\ell \in \{25, 50, 100, 200, 400, 800\}$. The step-sizes $(h, k) = (0.05, 4\text{e}-04)$ are considered fixed and the spatial points are $z_i = ih$, $1 \le i \le M - 1 = 19$ in the spatial domain $[0, 1]$. Plot (a): Successive absolute deviations (74) of the mean of the approximate concentration s.p.: $\text{AbsDev}\left[\mu\left(v_{K_\ell K_{\ell+1}}(z, 1, \omega)\right)\right]$. Plot (b): Successive absolute deviations (74) for the standard deviation of the approximate concentration s.p.: $\text{AbsDev}\left[\sigma\left(v_{K_\ell K_{\ell+1}}(z, 1, \omega)\right)\right]$.

Table 10
Maximum values of the absolute deviations for both statistical moments (76) of the approximate concentration s.p. over time $\tau = 1$. The step-sizes $(h_\ell, k_\ell) \in \{(0.1, 1.5\text{e}-03), (0.05, 4\text{e}-04), (0.025, 1\text{e}-04), (0.0125, 2.6\text{e}-05), (0.00625, 6.6\text{e}-06)\}$ are refined whereas the number of the Monte Carlo realizations is the fixed value $K = 100$. The values M and N are the spatial and temporal levels, respectively.

$\{h_\ell, h_{\ell+1}\}$	$\left\|\text{AbsDev}\left[\mu\left(v_{K,h_\ell,h_{\ell+1}}(z_i,\tau,\omega)\right)\right]\right\|_\infty$	$\left\|\text{AbsDev}\left[\sigma\left(v_{K,h_\ell,h_{\ell+1}}(z_i,\tau,\omega)\right)\right]\right\|_\infty$
{0.1, 0.05}	1.4270e − 05	4.3763e − 06
{0.05, 0.025}	9.9408e − 06	2.9493e − 06
{0.025, 0.0125}	4.8485e − 06	1.4057e − 06
{0.0125, 0.00625}	2.5455e − 06	7.2469e − 07

several time instants $\tau = \{0.1, 0.3, 0.5, 0.7\}$ together with the points where the mean of the interface s.p. is located in the spatial axe. In these simulations we have considered $K = 800$ Monte Carlo realizations and the step-sizes $(h, k) = (0.05, 4\text{e}-04)$.

4. Conclusions

Assuming uncertainty of the values of parameters in partial differential models turns them into random partial differential problems. To the best of our knowledge, this study seems to be the first time about moving boundary random Stefan problems in the mean square framework. In these problems not only the numerical solution of the unknown magnitude as concentration or temperature stochastic process needs to be obtained but also the approximation of the moving interface stochastic process. Inspired in the deterministic case where the front-fixing

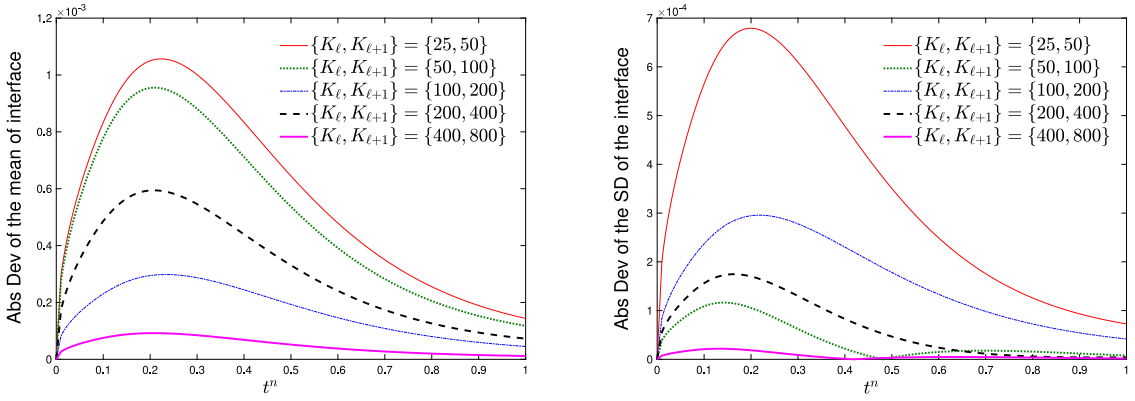

(a) (b)

Fig. 10. Absolute deviations over the time $\tau = 1$ for both statistical moments of the approximate interface s.p. between two successive realizations $\{K_\ell, K_{\ell+1}\}$, $K_\ell \in \{25, 50, 100, 200, 400, 800\}$. The step-sizes $(h, k) = (0.05, 4\text{e}-04)$ are considered fixed and the temporal points are $t^n = t^0 + nk$, $t^0 = 0.01$, $0 \le n \le N = 2475$, in the temporal domain $[0, \tau = 1]$. Plot (a): Successive absolute differences (75) for the mean of the approximate interface s.p.: AbsDev $\left[\mu\left(s_{K_\ell,K_{\ell+1}}(t^n,\omega)\right)\right]$. Plot (b): Successive absolute differences (75) for the standard deviation of the approximate interface s.p.: AbsDev $\left[\sigma\left(s_{K_\ell,K_{\ell+1}}(t^n,\omega)\right)\right]$.

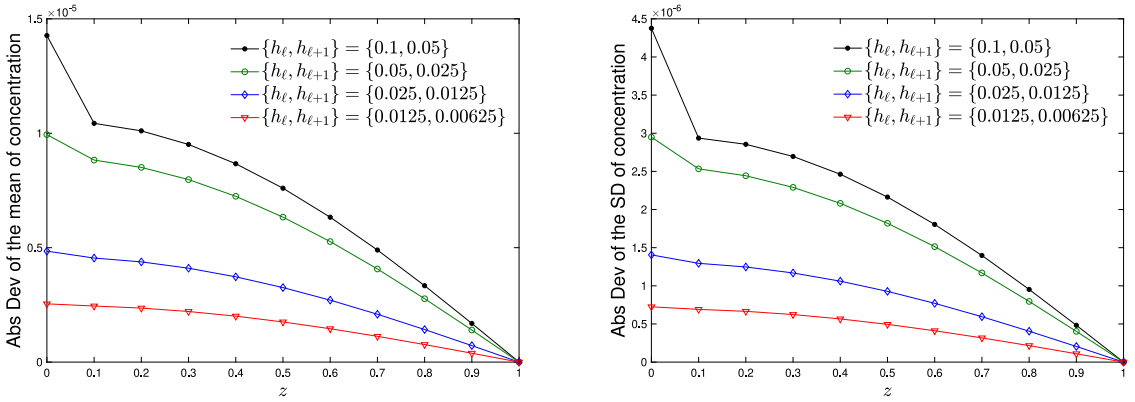

(a) (b)

Fig. 11. Absolute deviations over time $\tau = 1$ for both statistical moments of the approximate concentration s.p. for $K = 100$ Monte Carlo simulations and considering successive spatial step-sizes $\{h_\ell, h_{\ell+1}\}$, $h_\ell \in \{0.1, 0.05, 0.025, 0.0125, 0.00625\}$ with their corresponding time step-sizes $k_\ell \in \{1.5\text{e}-03, 4\text{e}-04, 1\text{e}-04, 2.6\text{e}-05, 6.6\text{e}-06\}$. Plot (a): Absolute deviation of the mean of the approximate concentration s.p. (76).: AbsDev $\left[\mu\left(v_{K,h_\ell,h_{\ell+1}}(z,1,\omega)\right)\right]$ Plot (b): Absolute deviation of the standard deviation of the approximate concentration s.p. (76).: AbsDev $\left[\sigma\left(v_{K,h_\ell,h_{\ell+1}}(z,1,\omega)\right)\right]$.

transformation allows to fix the spatial domain and incorporates the interface as a part of the derived transformed non-linear problem, we develop a random front-fixing method. For solving the transformed problem we propose a random explicit finite difference scheme providing the numerical analysis to guarantee qualitative properties of the solution such as stability, positivity and monotonicity. Monte Carlo technique provides a useful technique to manage the complexity of the moving boundary random problem in order to give numerical answer to the unknown mean and standard deviation of the involved approximating stochastic process. Future studies will focus in more complex random Stefan problems as two-phase ones.

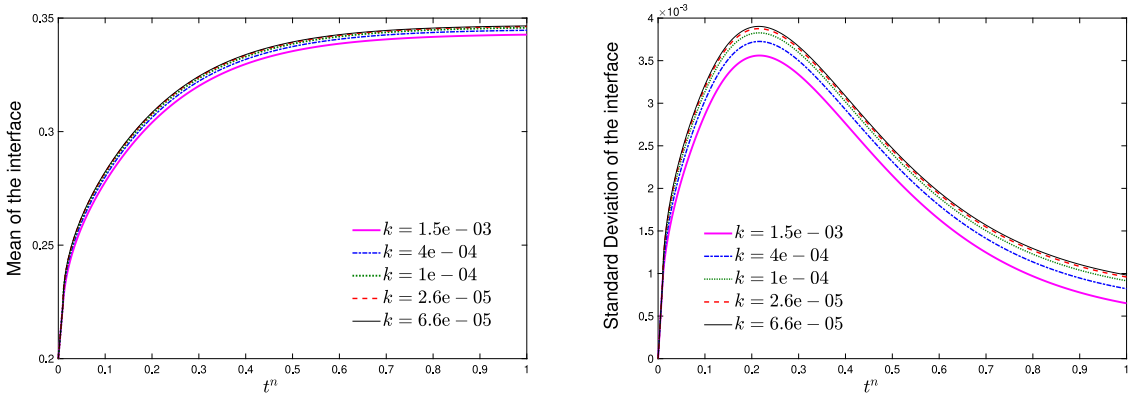

(a) (b)

Fig. 12. Evolution of both statistical moments of the interface s.p. along the time $\tau = 1$ refining the time step-size $k \in \{1.5e-03, 4e-04, 1e-04, 2.6e-05, 6.6e-05\}$ attending one to one the values of the spatial step-size $h \in \{0.1, 0.05, 0.025, 0.0125, 0.00625\}$ and considering $K = 100$ Monte Carlo simulations. Plot (a): The mean of the interface s.p. computed by (62): $\mu\left[s_K\left(t^n, \omega\right)\right]$. Plot (b): The standard deviation of the interface s.p. computed by (62): $\sigma\left[s_K\left(t^n, \omega\right)\right]$.

Table 11
Values of the mean $\mu\left(s_K(t^N, \omega)\right)$ and the standard deviation $\sigma\left(s_K(t^N, \omega)\right)$ of the interface s.p. in the last time instant $t^N = t^0 + Nk = 1$, $t^0 = 0.01$, for different time step-sizes k but fixing the number of realizations $K = 100$. Column μ-differences is the subtract between the consecutive values of $\mu\left(s_K(t^N, \omega)\right)$ and column σ-differences is the subtract between the consecutive values of $\sigma\left(s_K(t^N, \omega)\right)$.

(h, k)	(M, N)	$\mu\left(s_K(t^N, \omega)\right)$	μ-differences	$\sigma\left(s_K(t^N, \omega)\right)$	σ-differences
(0.1, 1.5e − 03)	(10, 660)	0.34270	–	6.5004e − 04	–
(0.05, 4e − 04)	(20, 2475)	0.34463	0.00193	8.2072e − 04	1.7068e − 04
(0.025, 1e − 04)	(20, 9900)	0.34575	0.00112	9.1462e − 04	9.3900e − 05
(0.0125, 2.6e − 05)	(40, 38077)	0.34628	0.00053	9.5896e − 04	4.4340e − 05
(0.00625, 6.6e − 05)	(160, 150000)	0.34655	0.00027	9.8227e − 04	2.3310e − 05

Table 12
CPU time seconds and their corresponding real time in seconds spent to compute both statistical moments at $\tau = 1$ with a fixed number of Monte Carlo realizations $K = 100$ as step-sizes (h, k) vary.

(h, k)	$[\mu/\sigma]\ (v_K(z_i, \tau, \omega), s_K(t^n, \omega))$ CPU, s	$[\mu/\sigma]\ (v_K(z_i, \tau, \omega), s_K(t^n, \omega))$ real time (seconds)
(0.1, 1.5e − 03)	0.4063	0.20
(0.05, 4e − 04)	1.1563	0.49
(0.025, 1e − 04)	4.0938	3.33
(0.0125, 2.6e − 05)	20.66	19.57
(0.00625, 6.6e − 06)	108	101.74

Financial support

This work was supported by the Spanish Ministerio de Economía, Industria y Competitividad (MINECO), Spain, the Agencia Estatal de Investigación (AEI), Spain and Fondo Europeo de Desarrollo Regional (FEDER UE) grant MTM2017-89664-P.

Ethics statement

This research did not require ethical approval.

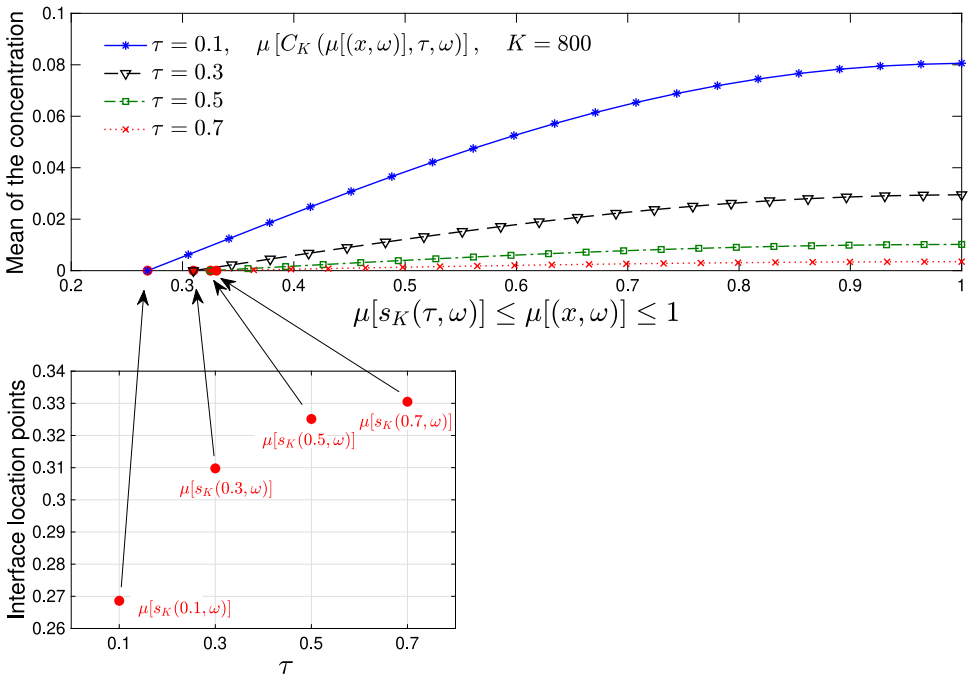

(a)

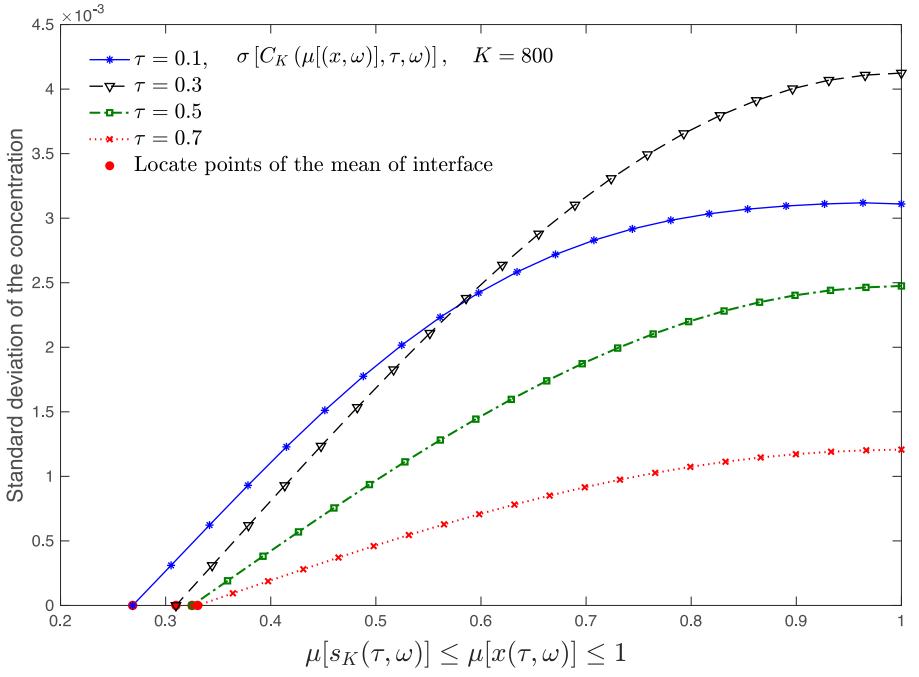

(b)

Fig. 13. Plot (a): Evolution of the mean of the concentration s.p. in several time instants $\tau = \{0.1, 0.3, 0.5, 0.7\}$. The red points in the spatial axe denote where the mean of the interface s.p. is located. (Bottom plot) Values of the mean of the interface s.p. in each time instant $\tau = \{0.1, 0.3, 0.5, 0.7\}$. Plot (b): Evolution of the standard deviation of the concentration s.p. and the locate of the mean of interface s.p. in the same time instants. In both graphics the Monte Carlo simulations are $K = 800$ and $(h, k) = (0.05, 4e-04)$.

Declaration of competing interest

The authors declare that they have no known competing financial interests or personal relationships that could have appeared to influence the work reported in this paper.

References

[1] S.G. Ahmed, A new semi-analytical method for phase transformation in binary alloys, J. Comput. Appl. Math. 206 (2007) 409–419.
[2] J. Caldwell, C.K. Chiu, Numerical solution of one-phase Stefan problems by the heat balance integral method, Part II-special small time starting procedure, Commun. Numer. Methods Eng. 16 (2000) 585–593.
[3] J. Caldwell, Y.Y. Kwan, Numerical methods for one-dimensional Stefan problems, Commun. Numer. Methods Eng. 20 (2004) 535–545.
[4] J. Caldwell, S. Savović, Numerical solution of Stefan problem by variable space grid and boundary immobilization method, J. Math. Sci. 13 (2002) 67–79.
[5] M.-C. Casabán, R. Company, L. Jódar, Reliable efficient difference methods for random heterogeneous diffusion reaction models with a finite degree of randomness, Mathematics 9 (2021) 206.
[6] J. Crank, Free and Moving Boundary Problems, Clarendon Press, Oxford, 1984.
[7] T. Dokoza, D. Plümacher, M. Smuda, C. Jegust, M. Oberlack, Solution to the 1D Stefan problem using the unified transform method, J. Phys. A 54 (2021) 375203.
[8] E. Javierre, C. Vuik, F.J. Vermolen, A. Segal, A Level Set Method for Particle Dissolution in a Binary Alloy. Report at the Delft Institute of Applied Mathematics (2005) 03–05.
[9] E. Javierre, C. Vuik, F.J. Vermolen, S. Van der Zwaag, A comparison of numerical models for one-dimensional Stefan problems, J. Comput. Appl. Math. 192 (2006) 445–459.
[10] M. Keller-Ressel, M.S. Müller, A Stefan-type stochastic moving boundary problem, Stoch. PDE: Anal. Comp. 4 (2016) 746–790.
[11] H. Landau, Heat conduction in a melting solid, Quart. Appl. Math. 8 (1950) 81–95.
[12] S.L. Mitchell, M. Vynnycky, On the accurate numerical solution of a two-phase Stefan problem with phase formation and depletion, J. Comput. Appl. Math. 300 (2016) 259–274.
[13] M.S. Müller, Approximation of the interface condition for stochastic Stefan-type problems, Discrete Contin. Dyn. Syst. Ser. B 24 (8) (2019) 4317–4339.
[14] M. Ögren, Stochastic solutions of Stefan problems, 2000, http://dx.doi.org/10.48550/arXiv.2006.04939, arXiv:2006.04939.
[15] B. Øksendal, Stochastic Differential Equations, An Introduction with Applications, fifth ed., Springer, Berlin, Heildelberg, 2010.
[16] M.-A. Piqueras, R. Company, L. Jódar, A front-fixing numerical method for a free boundary nonlinear diffusion logistic population model, J. Comput. Appl. Math. 309 (2017) 473–481.
[17] M.-A. Piqueras, R. Company, L. Jódar, Solving two-phase freezing Stefan problems: Stability and monotonicity, Math. Methods Appl. Sci. 43 (2020) 7948–7960.
[18] J.A. Riddick, W.B. Bunger, Organic Solvents: Physical Properties and Methods of Purification, third ed., Wiley Interscience, New York, 1970.
[19] S. Savović, J. Caldwell, Finite difference solution of one-dimensional Stefan problem with periodic boundary conditions, Int. J. Heat Mass Transfer 46 (15) (2003) 2911–2916.
[20] G. Segal, C. Vuik, F. Vermolen, A conserving discretization for the free boundary in a two-dimensional Stefan problems, J. Comput. Phys. 114 (1994) 146–159.
[21] K.A. Sharp, Water: structure and properties in eLS, 2001.
[22] T.T. Soong, Random Differential Equations in Science and Engineering, Academic Press, New York, NY, USA, 1973.
[23] L. Villafuerte, C.A. Braumann, J.-C. Cortés, L. Jódar, Random differential operational calculus: Theory and applications, Comput. Math. Appl. 59 (2010) 115–125.
[24] L. Wu, Y.-K. Kwok, A front-fixing method for the valuation of American option, J. Financ. Eng. 6 (2) (1997) 83–97.